Recent results on hadrons at Belle and Belle II experiments

Chengping Shen (Fudan University)

第八届手征有效场论研讨会,
河南大学, 2023年10月27日至10月31日

logo designed by undergraduate student…

asymmetric e^+e^- collider
producing B mesons

$\Upsilon(4S)$ B-factory

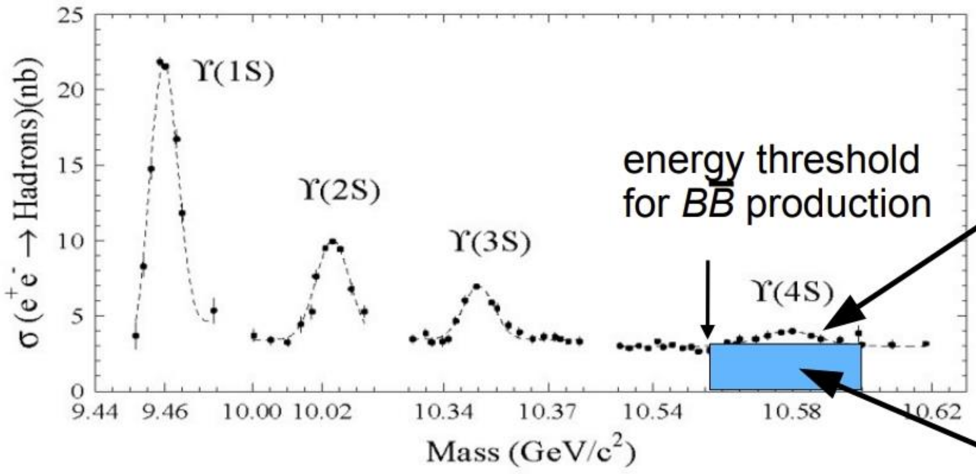

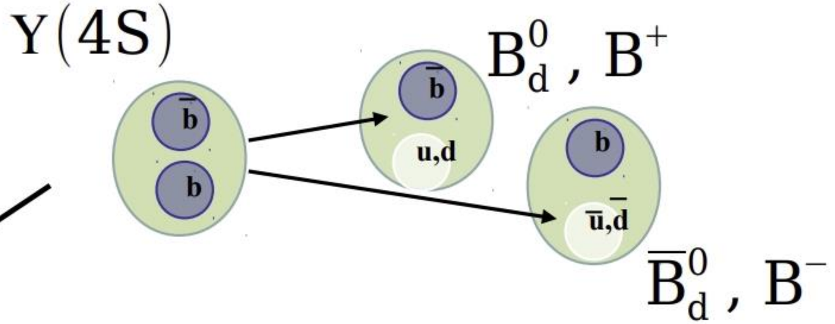

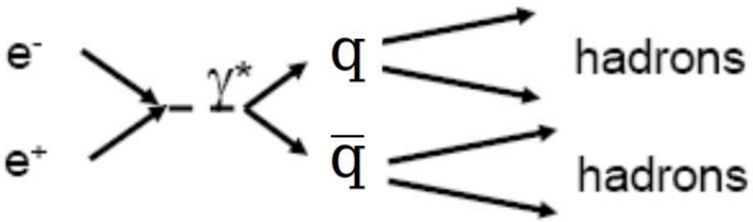

- **"on resonance" production**
  $e^+e^- \rightarrow \Upsilon(4S) \rightarrow B_d^0\bar{B}_d^0,\ B^+B^-$
  $\sigma(e^+e^- \rightarrow B\bar{B}) \simeq 1.1$ nb

- **"continuum" production ($q\bar{q} = u\bar{u},\ d\bar{d},\ s\bar{s},\ c\bar{c}$)**
  $\sigma(e^+e^- \rightarrow c\bar{c}) = 1.3$ nb
  $\sigma(e^+e^- \rightarrow s\bar{s}) = 0.4$ nb
  $\sigma(e^+e^- \rightarrow u\bar{u}) = 1.6$ nb
  $\sigma(e^+e^- \rightarrow d\bar{d}) = 0.4$ nb

- **$\sigma(e^+e^- \rightarrow \tau^+\tau^-) \sim 1$ nb**
- **$\sigma(e^+e^- \rightarrow \mu^+\mu^-) \sim 1$ nb (calibration)**
- **bhabha: $\sigma(e^+e^- \rightarrow e^+e^-) \sim 100$ nb (luminosity)**

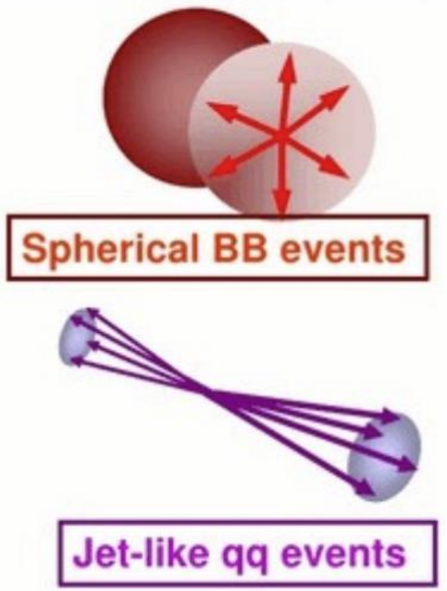

Belle(II), LHCb side by side

Belle (II)	LHCb
$e^+e^- \rightarrow \Upsilon(4S) \rightarrow b\bar{b}$	$pp \rightarrow b\bar{b}X$
at $\Upsilon(4S)$: 2 B's (B^0 or B^+) and nothing else ⇒ clean events (flavour tagging, B tagging, missing energy)	production of B^+, B^0, B_s, B_c, Λ_b... but also a lot of other particles in the event ⇒ lower reconstruction efficiencies
⇒ initial conditions are precisely known	$\sigma_{b\bar{b}}$ much higher than at the $\Upsilon(4S)$
$\sigma_{b\bar{b}} \sim 1\,nb \Rightarrow 1\ fb^{-1}$ produces $10^6\ B\bar{B}$ $\sigma_{b\bar{b}}/\sigma_{total} \sim 1/4$	

	$\sqrt{s}$ [GeV]	$\sigma_{b\bar{b}}$ [nb]	$\sigma_{b\bar{b}} / \sigma_{tot}$
HERA pA	42 GeV	~30	~10^{-6}
Tevatron	2 TeV	5000	~10^{-3}
LHC	8 TeV	~$3x10^5$	~ $5x10^{-3}$
	14 TeV	~$6x10^5$	~10^{-2}

$b\bar{b}$ production cross-section at LHCb ~ 500,000 × BaBar/Belle !!

Belle (II)	LHCb
higher luminosity	$\sigma_{b\bar{b}}/\sigma_{total}$ much lower than at the $\Upsilon(4S)$ ⇒ lower trigger efficiencies

B mesons live relativey long

Belle (II)	LHCb
mean decay length $\beta\gamma c\tau \sim 200\ \mu m$	**mean decay length $\beta\gamma c\tau \sim 7$ mm** (displaced vertices)

data taking period(s)

Belle (II)	LHCb
[1999-2010] = 1 ab^{-1} [2019-...] = ...	[run I: 2010-2012] = 3 fb^{-1} [run II: 2015-2018] = 6 fb^{-1}

(near) future

Belle (II)	LHCb
[Belle II from 2019] → 50 ab^{-1}	[LHCb upgrade from 2022]

A diversified physics program

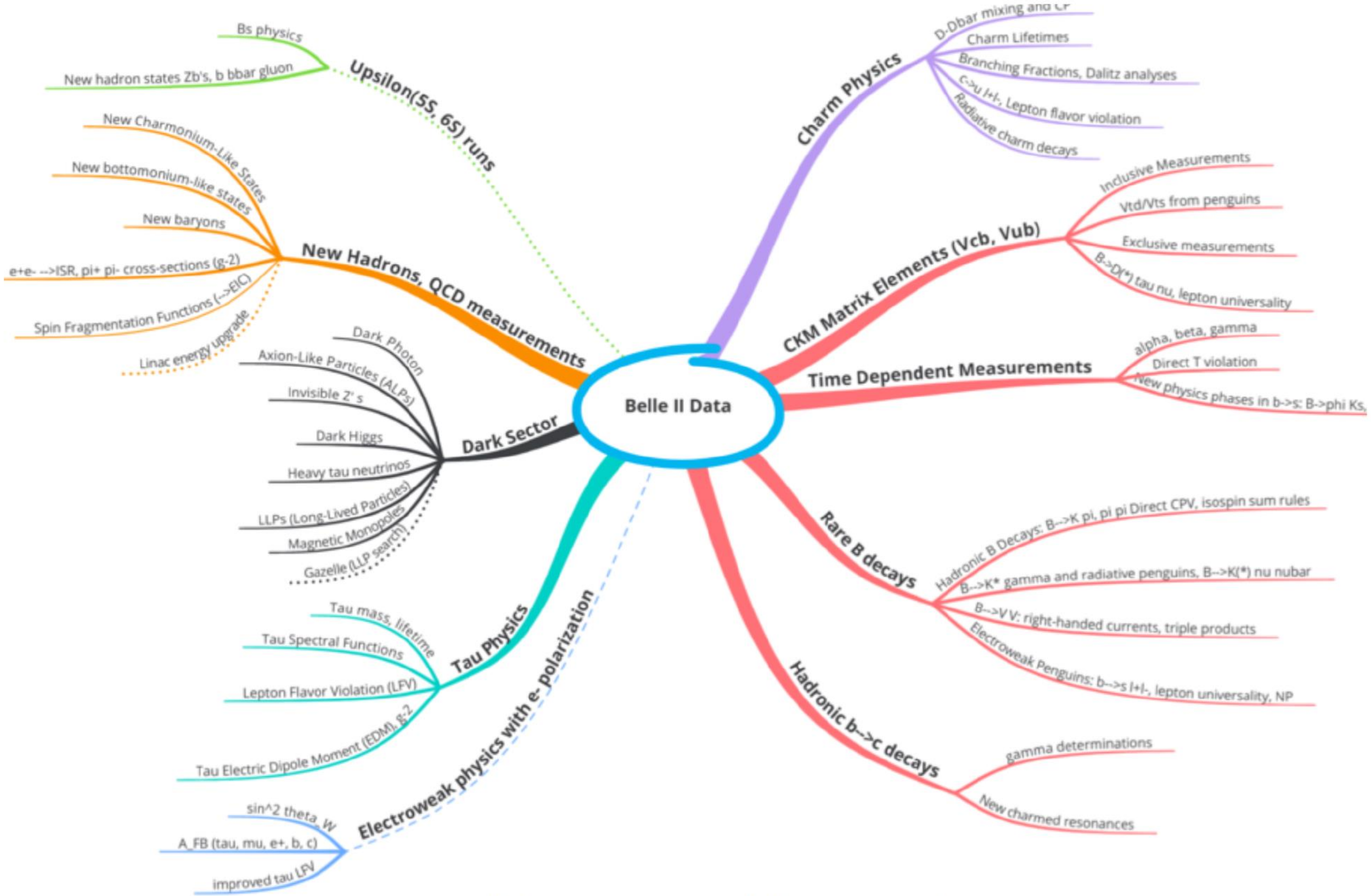

[Snowmass white paper]

Due to the time limitation, today I mainly focused on the quarkonium, charmed baryons, exotic states,… from Belle and Belle II.

PTEP 2019 123C01

From KEKB to SuperKEKB

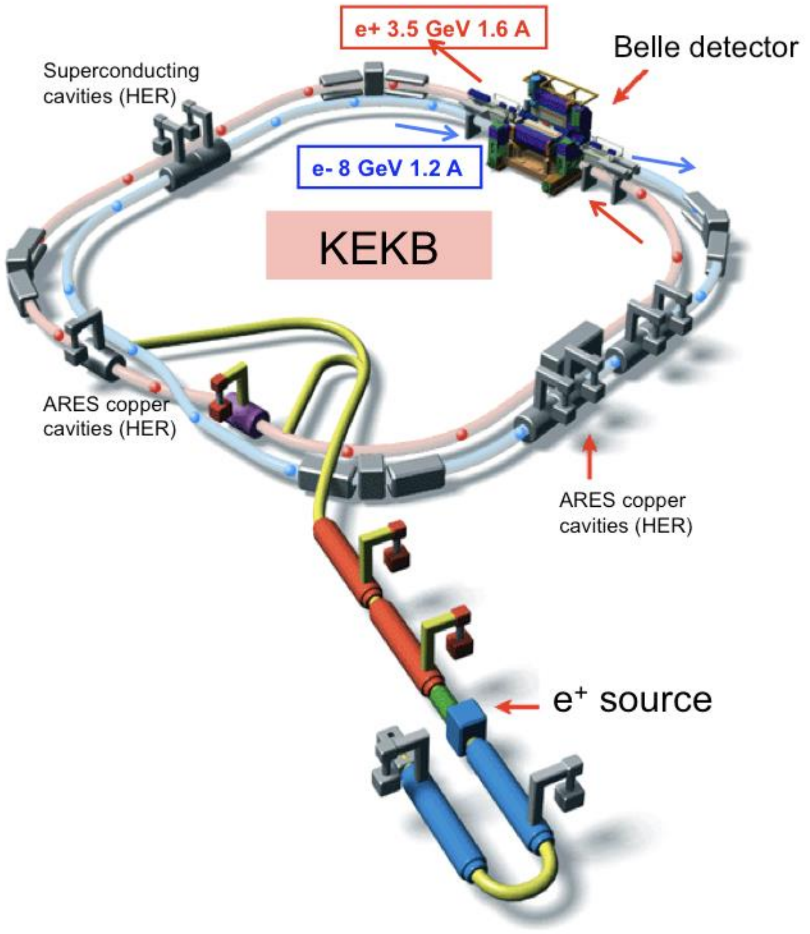

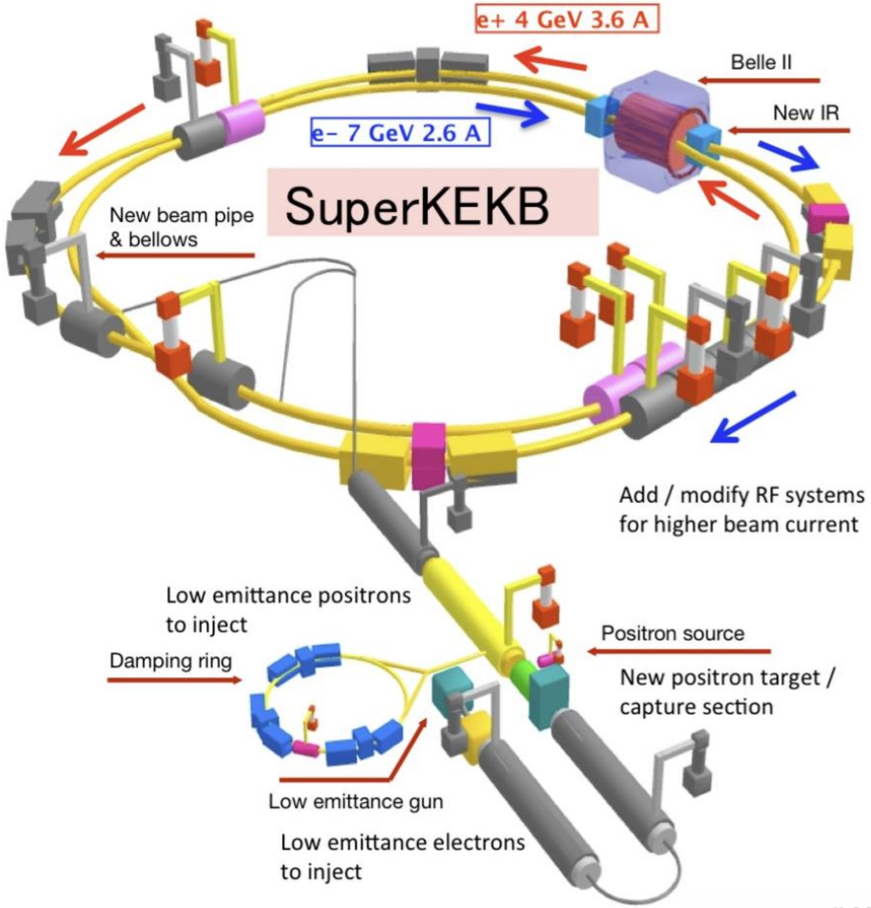

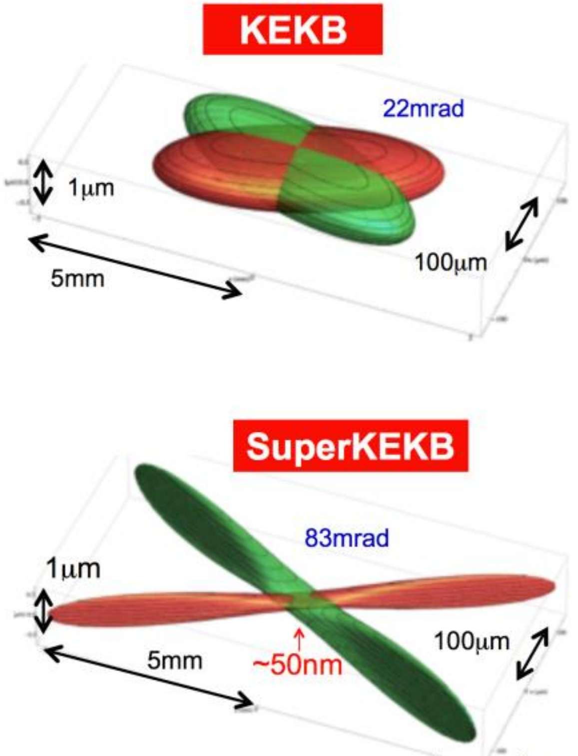

$$\mathcal{L} = \frac{\gamma_\pm}{2er_e}\left(1+\frac{\sigma_y^*}{\sigma_x^*}\right)\frac{I_\pm \xi_{y\pm}}{\beta_{y\pm}^*}\left(\frac{R_L}{R_{\xi_y}}\right)$$

- **moderately increased beam currents**
- **Squeeze beams @IP by ~1/20**

$$\mathcal{L}_{\mathrm{II}}^{\mathrm{peak}} \approx 30 \times \mathcal{L}_{\mathrm{I}}^{\mathrm{peak}}$$

$$\int^{\mathrm{goal}} \mathcal{L}_{\mathrm{II}}\, dt = 50\ \mathrm{ab}^{-1} \approx 50 \int \mathcal{L}_{\mathrm{I}}\, dt$$

Belle II detector
Vs.
Belle detector

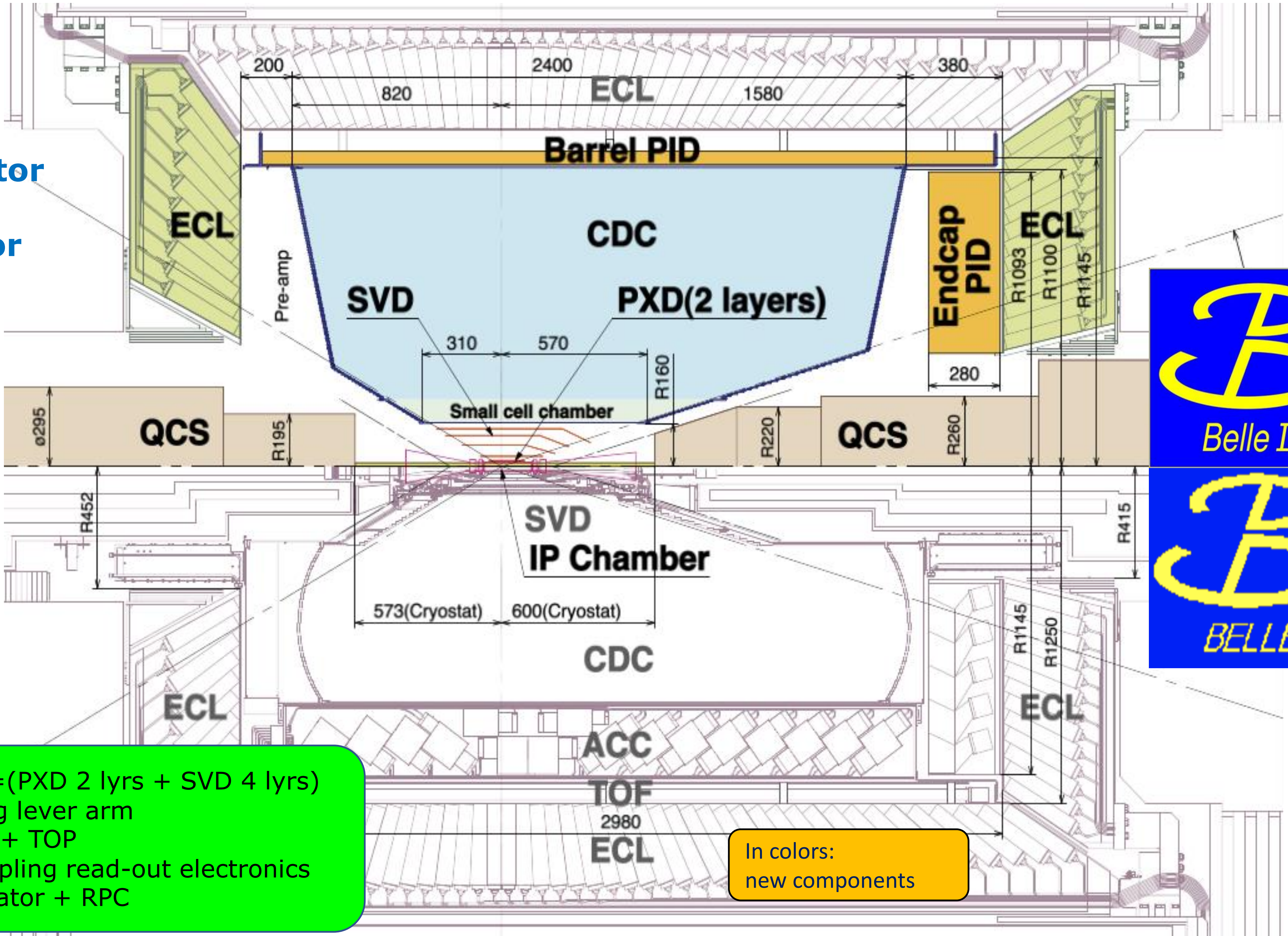

SVD: 4 lyrs → VXD=(PXD 2 lyrs + SVD 4 lyrs)
CDC: small cell, long lever arm
ACC+TOF → ARICH + TOP
ECL: waveform sampling read-out electronics
KLM: RPC → Scintillator + RPC

In colors:
new components

Datasets at Belle and Belle II

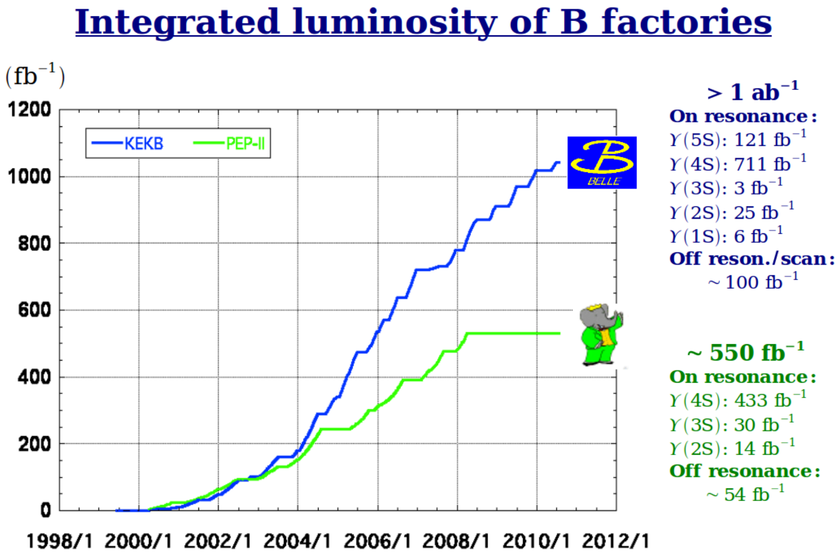

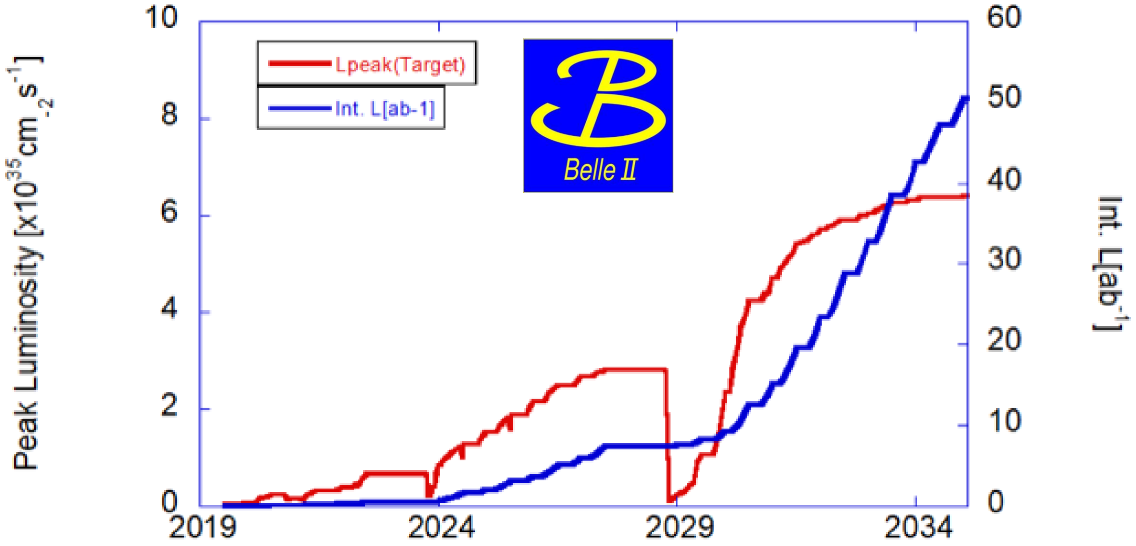

Data taking: 1999 – 2010

On/off/Scan Υ(nS) peaks

772M $B\bar{B}$ events @Υ(4S)

- Collected ~424 fb^{-1} around Υ(4S) until now
- LS1 starts in summer 2022 to fully install the pixel detector and accelerator machine study
- Operation will be resumed around the end of 2023

Bottomonium

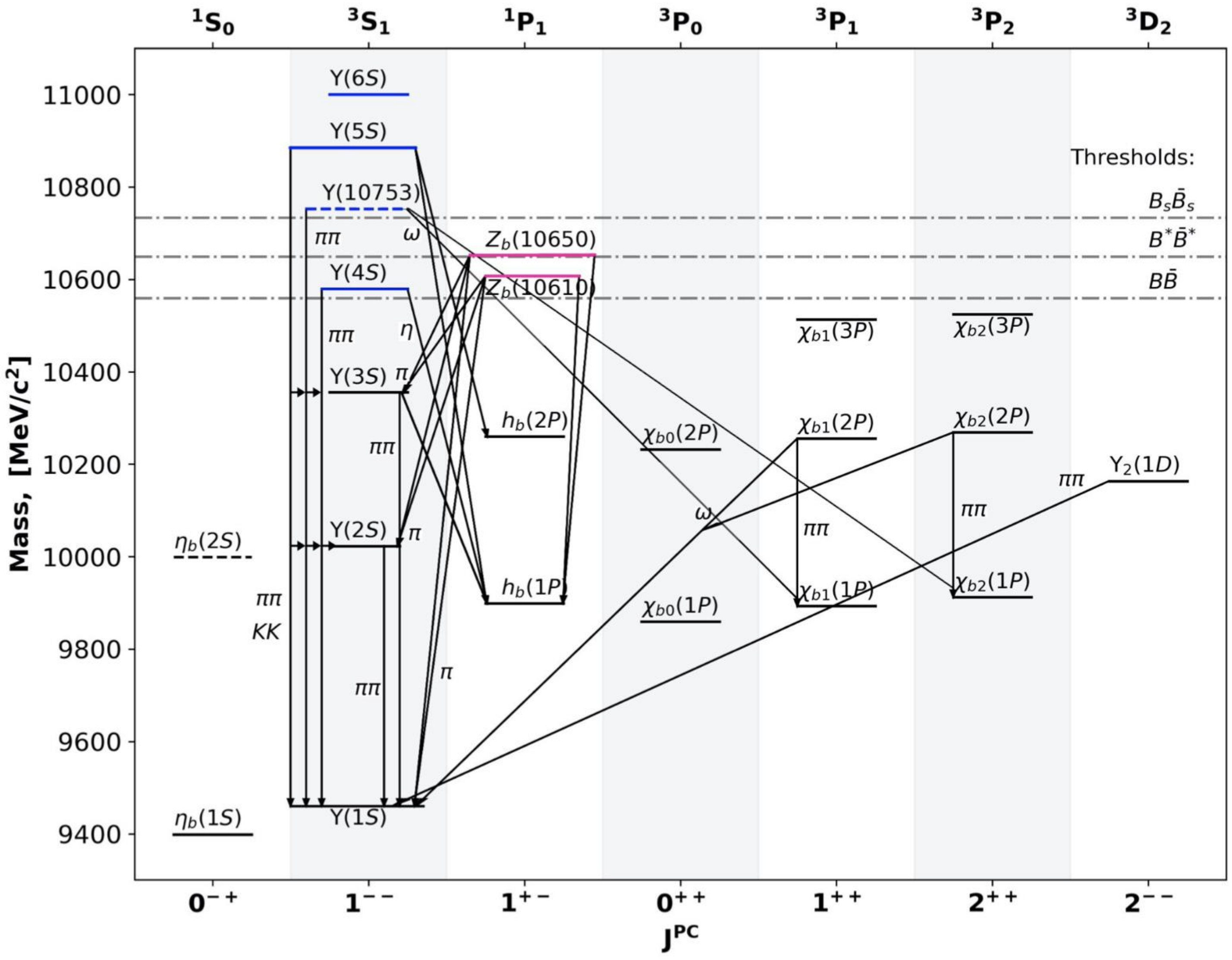

- Below $B\bar{B}$ thresholds – bottomonia are well described by the potential models.
- Above $B\bar{B}$ thresholds – bottomonia express unexpected properties:

- Two charged Z_b^+ states are observed ($B^{(*)}\bar{B}^*$ molecular?)
- Hadronic transitions are strongly enhanced (OZI rule violation);
- η transitions are not suppressed compare to $\pi^+\pi^-$ transitions (heavy quark spin-symmetry violation);

Conventional bottomonium (pure $b\bar{b}$ states)
Bottomonium-like states (mix of $b\bar{b}$ and $B\bar{B}$)
Exotic charged states (Z_b^+)

Discovery of $\Upsilon(10753)$

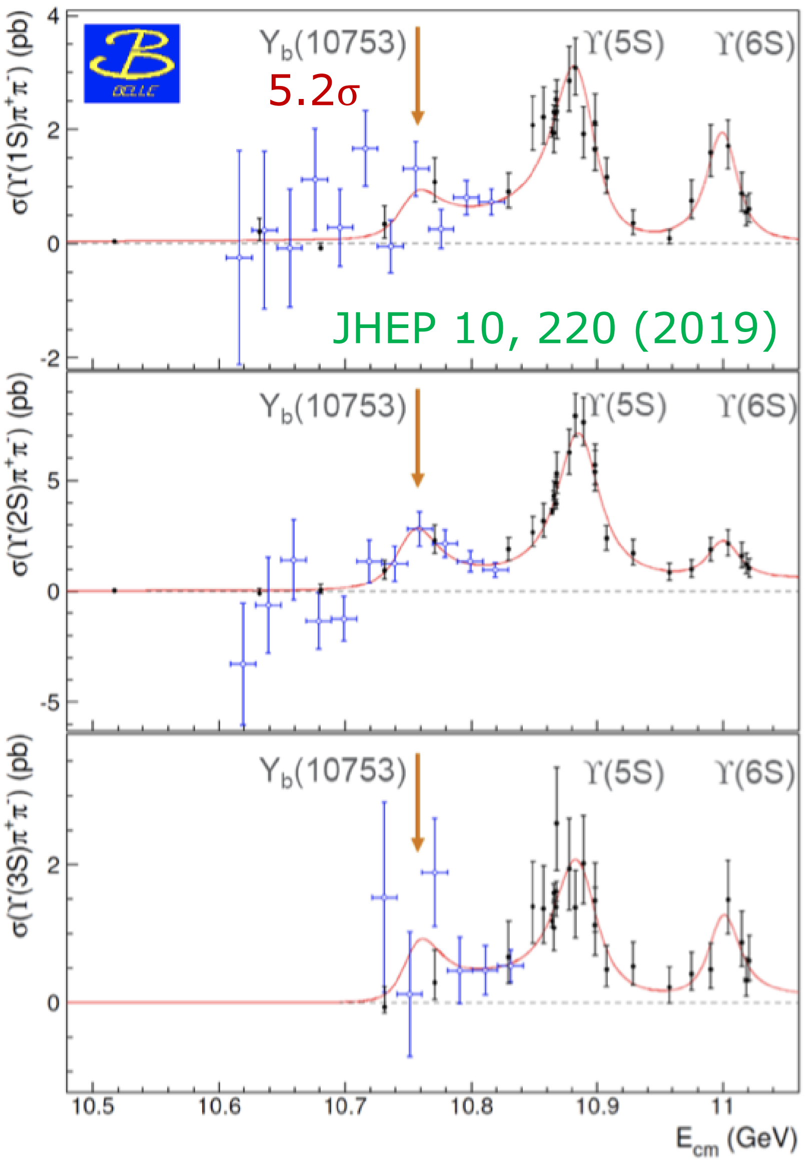

- Belle: several ~1fb^{-1} scan points below $\Upsilon(5S)$
- New structure observed in $\pi^+\pi^-\Upsilon(nS)$ transitions

	$\Upsilon(10860)$	$\Upsilon(11020)$	New structure
M (MeV/c^2)	$10885.3 \pm 1.5\,^{+2.2}_{-0.9}$	$11000.0^{+4.0}_{-4.5}\,^{+1.0}_{-1.3}$	$10752.7 \pm 5.9\,^{+0.7}_{-1.1}$
Γ (MeV)	$36.6^{+4.5}_{-3.9}\,^{+0.5}_{-1.1}$	$23.8^{+8.0}_{-6.8}\,^{+0.7}_{-1.8}$	$35.5^{+17.6}_{-11.3}\,^{+3.9}_{-3.3}$

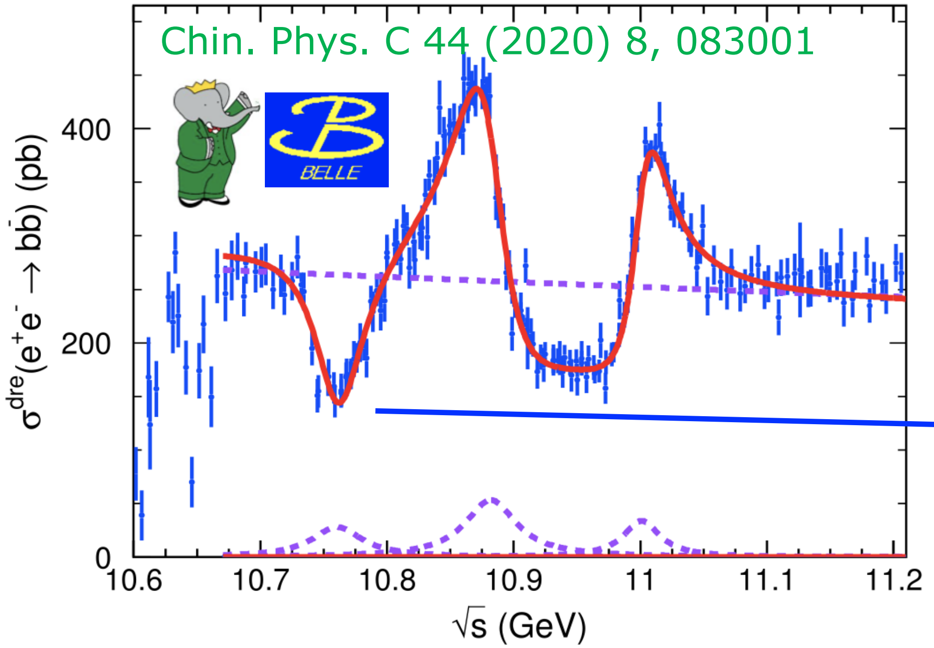

A dip at 10.75 GeV may correspond to $\Upsilon(10753)$.

Theoretical interpretations

Godfrey and Moats, PRD 92, 054034 (2015)

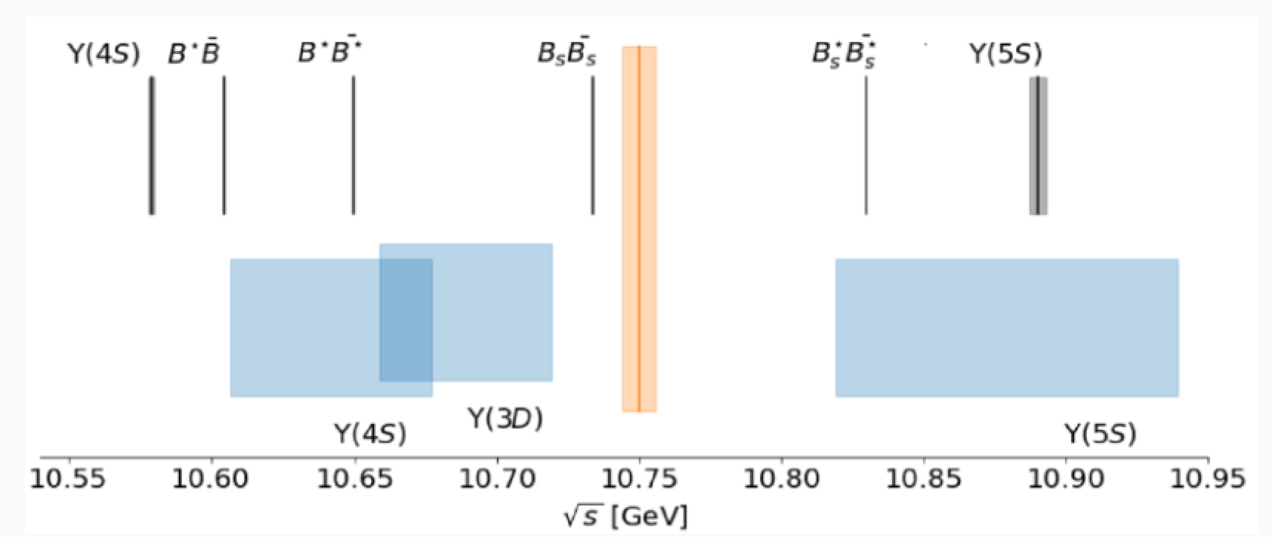

- Mass does not match ϒ(3D) theoretical predictions, and D-wave states are not seen in e^+e^- collisions.
- ϒ(4S) - ϒ(3D) mixing can be enhanced due to hadron loops.

❑ Conventional bottomonium

Eur. Phys. J. C 80, 59 (2020)
Phys. Rev. D 101, 014020 (2020)
Phys. Rev. D 102, 014036 (2020)
Phys. Lett. B 803, 135340 (2020)
Phys. Rev. D 104, 034036 (2021)
Prog. Part. Nucl. Phys. 117, 103845 (2021)
Eur. Phys. J. Plus 137, 357 (2022)
Phys. Rev. D 105, 114041 (2022)
Phys. Rev. D 106, 094013 (2022)
Phys. Rev. D 105, 074007 (2022)

❑ Hybrid

Phys. Rept. 873, 1 (2020)
Phys. Rev. D 104, 034019 (2021)

❑ Tetraquark

Chin. Phys. C 43, 123102 (2019)
Phys. Lett. B 802, 135217 (2020)
Phys. Rev. D 103, 074507 (2021)
Phys. Rev. D 107, 094515 (2023)

Unique scan data near $\sqrt{s} = 10.75$ GeV

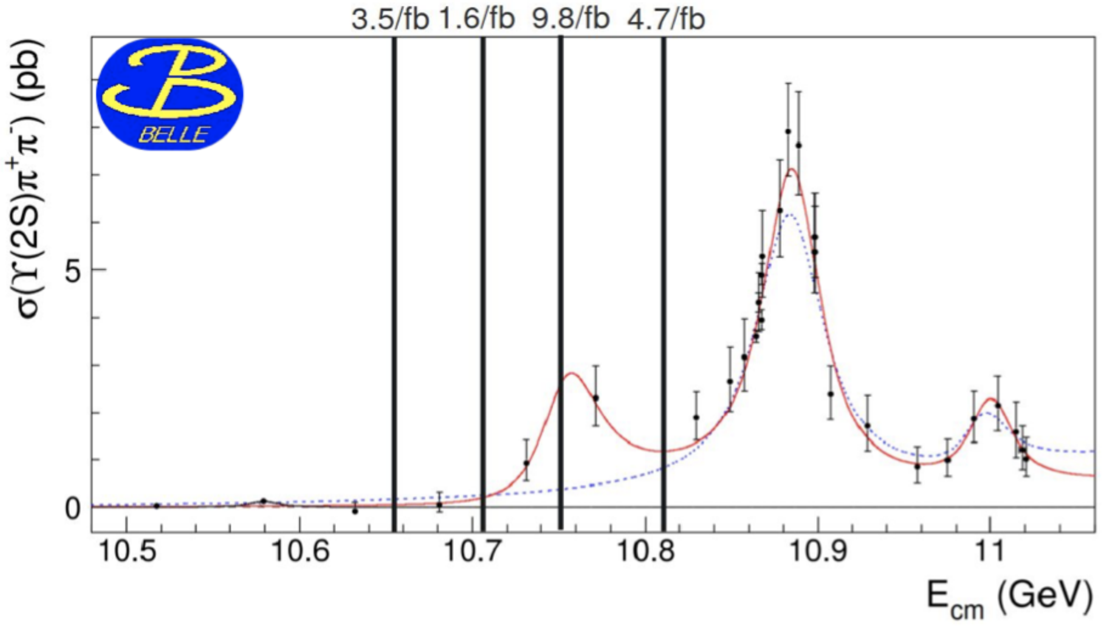

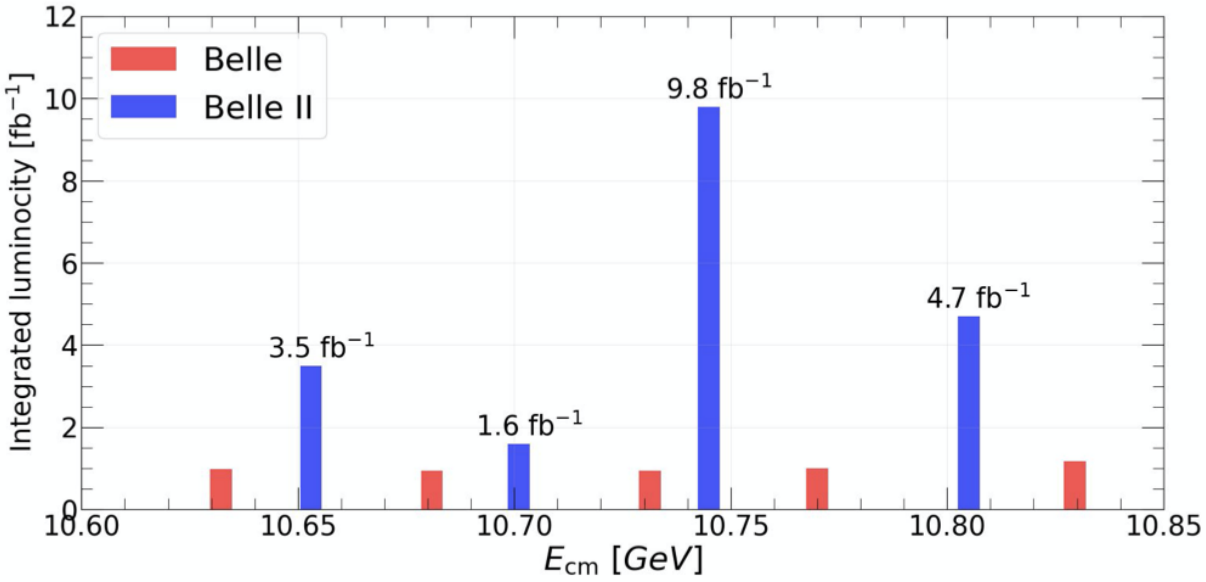

- In November 2021, Belle II collected 19 fb^{-1} of unique data at energies above the ϒ(4S): four energy scan points around 10.75 GeV.
- Belle II collected the data in the gaps between Belle energy scan points.
- Physics goal: understand the nature of the ϒ(10753) energy region.

Motivation to search for $\Upsilon(10753) \to \omega\chi_{bJ}$

Theory: Branching fractions of 10^{-3} for $\Upsilon(10753) \to \omega\chi_{bJ}$ [PRD 104, 034036 (2021)] and $\Upsilon(10753) \to \pi^+\pi^-\Upsilon(nS)$ [PRD 105, 074007 (2022)] assuming $\Upsilon(4S)$ - $\Upsilon(3D)$ mixing state for $\Upsilon(10753)$.

Charmonium sector:

- Two close peaks observed in the cross sections for $e^+e^- \to \pi^+\pi^- J/\psi$ by BESIII and $e^+e^- \to \pi^+\pi^-\Upsilon(nS)$ by Belle, respectively, may suggest similar nature.
- Y(4220) $\to \gamma X(3872)$ and $\omega\chi_{c0}$ observed by BESIII.
- So we expect the observations of $\Upsilon(10753) \to \gamma X_b$ and $\omega\chi_{bJ}$.

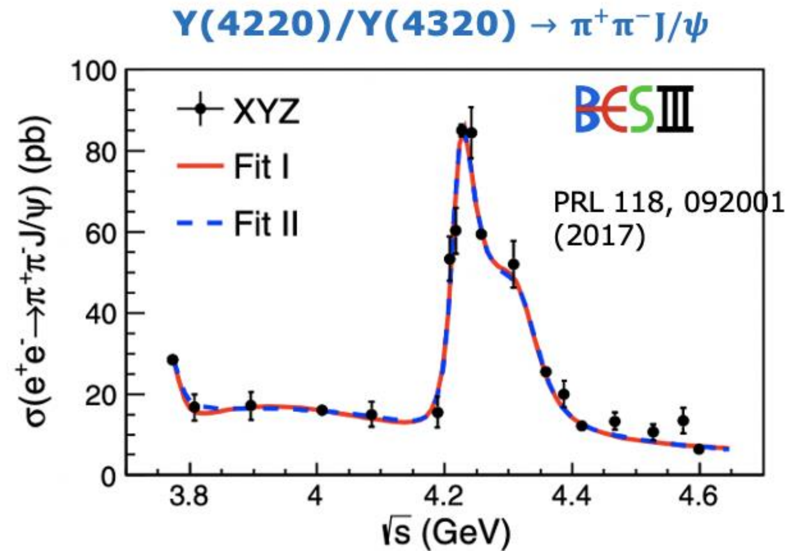

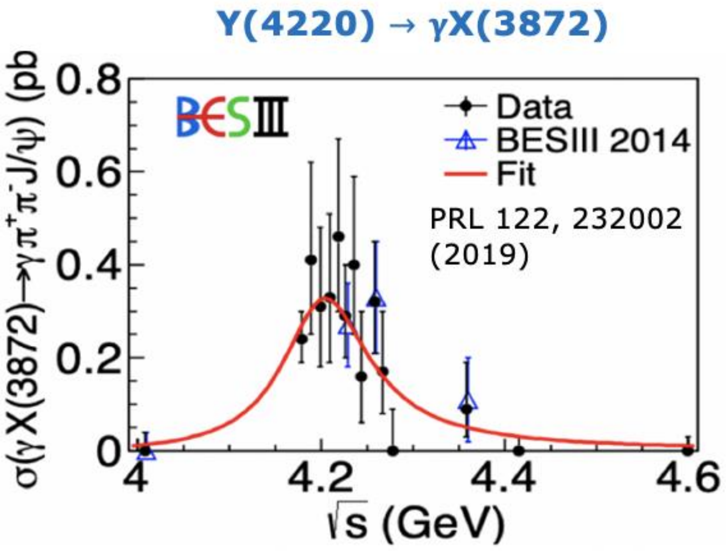

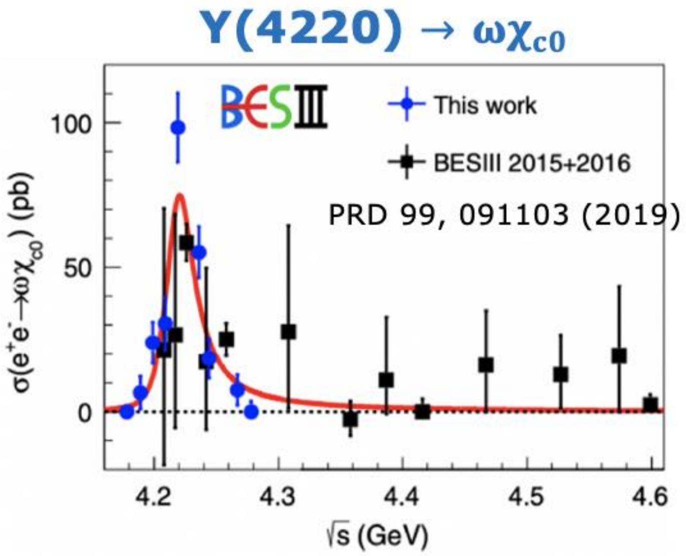

Observation of $\Upsilon(10753)\to\omega\chi_{bJ}$

PRL 130, 091902 (2023)

Two dimensional unbinned maximum likelihood fits to the $M(\gamma\Upsilon(1S))$ and $M(\pi^+\pi^-\pi^0)$ distributions.

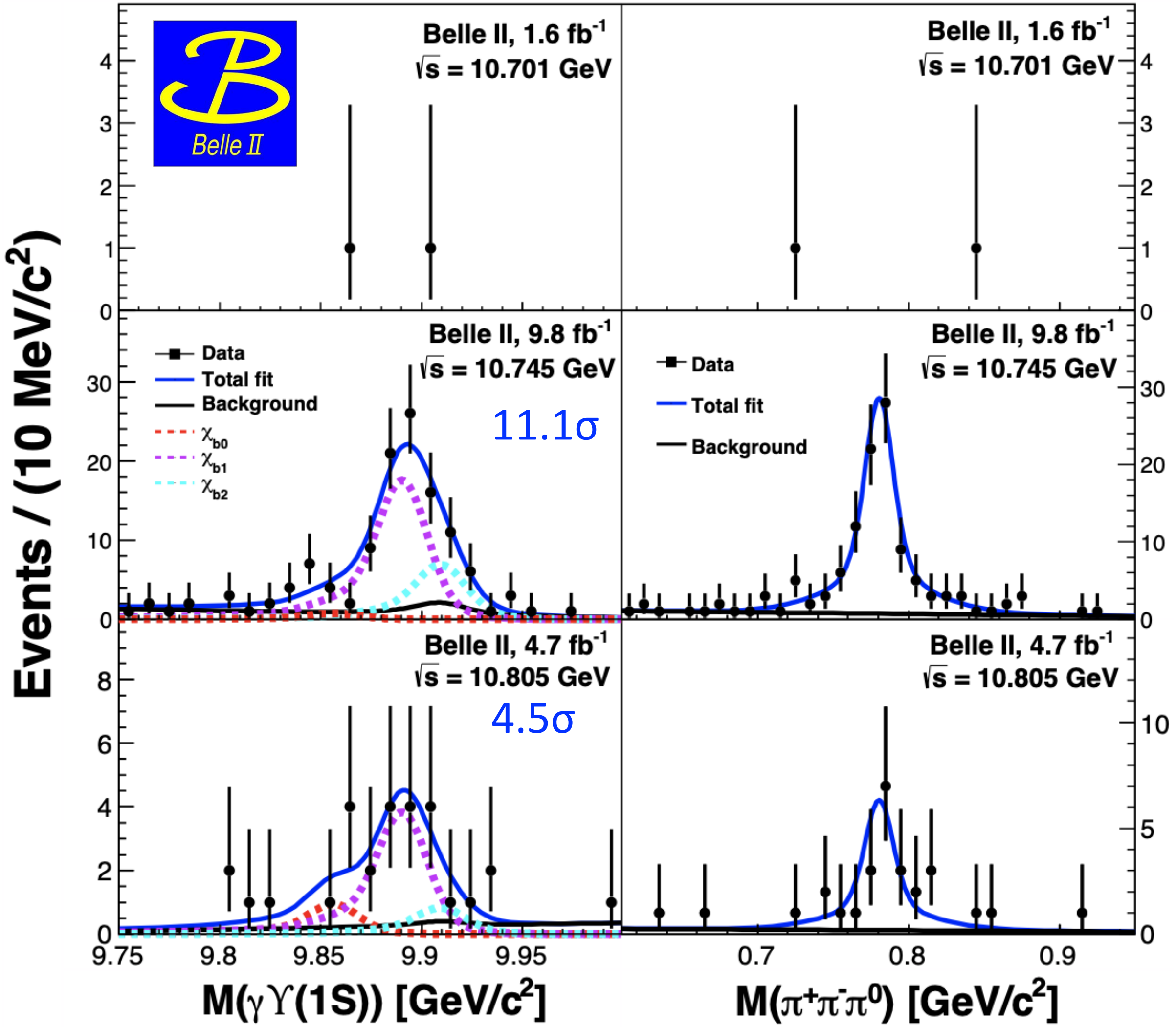

Channel	$\sqrt{s}$ (GeV)	N^{sig}	$\sigma_{Born}^{(UL)}$ (pb)
$\omega\chi_{b1}$	10.745	$68.9^{+13.7}_{-13.5}$	$3.6^{+0.7}_{-0.7}\pm0.4$
$\omega\chi_{b2}$		$27.6^{+11.6}_{-10.0}$	$2.8^{+1.2}_{-1.0}\pm0.5$
$\omega\chi_{b1}$	10.805	$15.0^{+6.8}_{-6.2}$	1.6 @90% C.L.
$\omega\chi_{b2}$		$3.3^{+5.3}_{-3.8}$	1.5 @90% C.L.

The $e^+e^-\to\omega\chi_{bJ}$ (J = 1, 2) cross sections peak at $\Upsilon(10753)$.

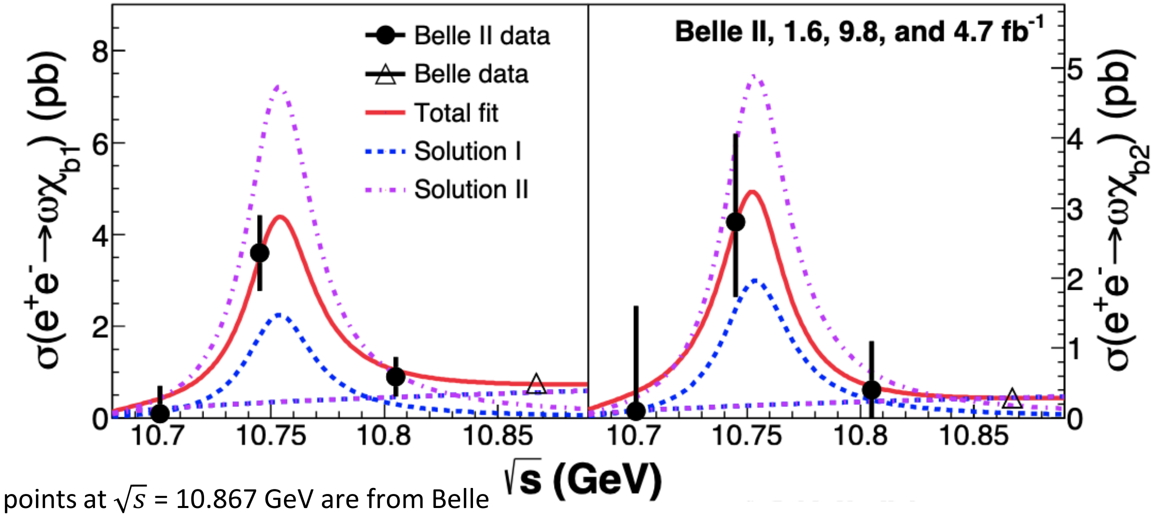

The points at $\sqrt{s}$ = 10.867 GeV are from Belle measurements [PRL 113, 142001 (2014)].

Discussion

$$\frac{\sigma(e^+e^-\to\chi_{bJ}(1P)\omega)}{\sigma(e^+e^-\to\Upsilon(nS)\pi^+\pi^-)} \sim$$

$\sim$1.5 at $\sqrt{s}$ = 10.745 GeV [PRL 130, 091902 (2023)]

$\sim$ 0.15 at $\sqrt{s}$ = 10.867 GeV [PRL 113, 142001 (2014)]

- ϒ(5S) and ϒ(10753) have same quantum numbers and similar masses, but the difference on the above ratio is large. This may indicate **the difference in the internal structures of these two states**.

$$\frac{\sigma(e^+e^-\to\chi_{b1}(1P)\omega)}{\sigma(e^+e^-\to\chi_{b2}(1P)\omega)} = 1.3\pm0.6 \text{ at } \sqrt{s} = 10.745 \text{ GeV [PRL 130, 091902 (2023)]}$$

- **Contradicts the expectation for a pure D−wave bottomonium state of 15** [Phys. Lett. B 738, 172 (2014)]
- **An observation of 1.8σ difference with the prediction for a S−D−mixed state of 0.2** [Phys. Rev. D 104, 034036 (2021)]

Search for X_b

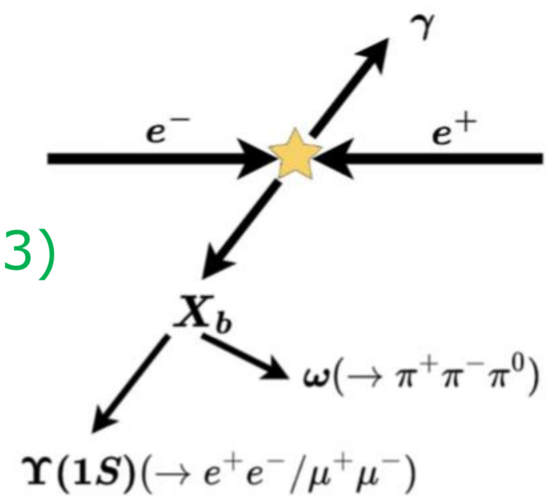

PRL 130, 091902 (2023)

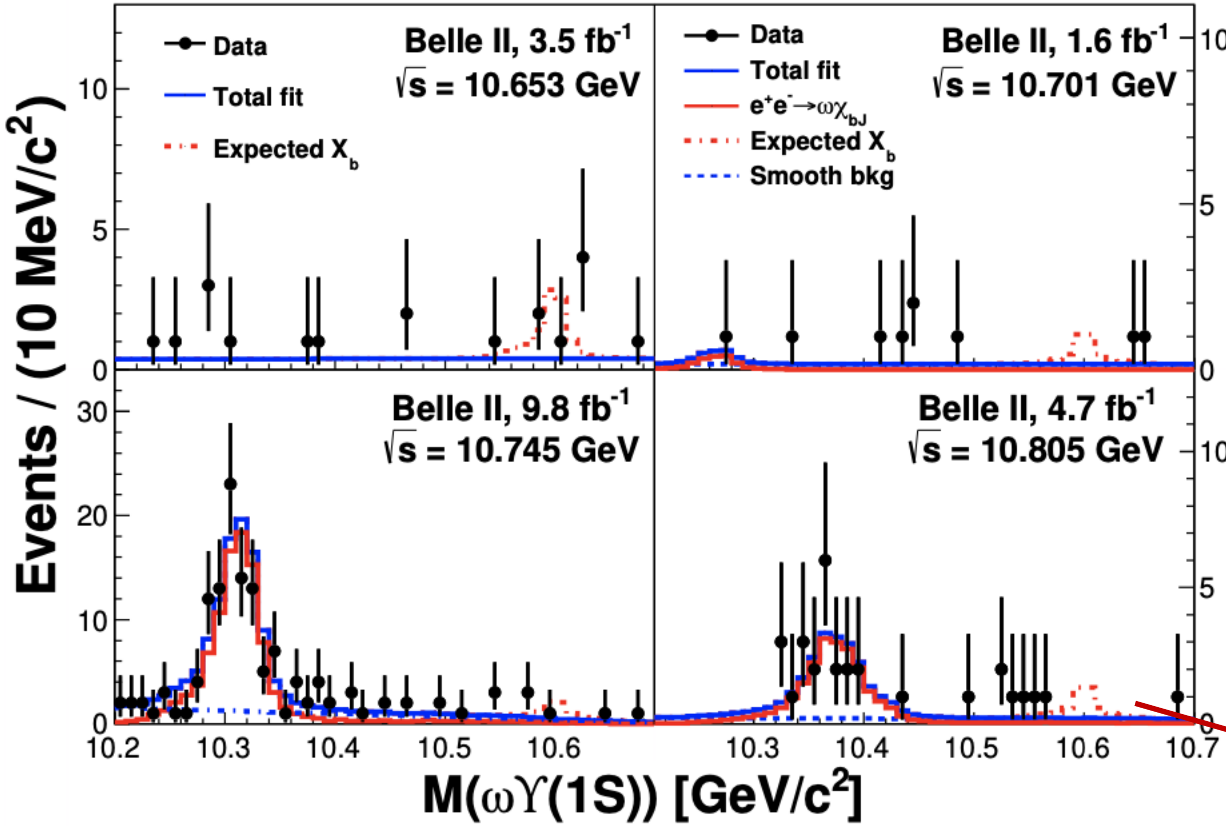

- No significant X_b signal is observed.
- The peaks are the reflections of $e^+e^- \to \omega\chi_{bJ}$.

From simulated events with $m(X_b)$ = 10.6 GeV/c²
The yield is fixed at the upper limit at 90% C.L.

Upper limits at 90% C.L. on $\sigma_B(e^+e^- \to \gamma X_b) \cdot \mathcal{B}(X_b \to \omega\Upsilon(1S))$ (pb)	$\sqrt{s}$ (GeV)	10.653	10.701	10.745	10.805
	$m(X_b)$ = 10.6 GeV/c²	0.46	0.33	0.10	0.14
	$m(X_b)$ = (10.45, 10.65) GeV/c²	(0.14, 0.55)	(0.25, 0.84)	(0.06, 0.14)	(0.08, 0.37)

Measurement of the energy dependence of the $e^+e^- \to B\bar{B}$, $B\bar{B}^*$ and $B^*\bar{B}^*$ cross sections

$\sqrt{s} = 10.745$ GeV, 9.8 fb^{-1}

- The $B^{(*)}\bar{B}^{(*)}$ are expected to be dominant decay channels for excited bottomonium-like states. Their measurements are critical for understanding these states.

Method:

One B meson is reconstructed in hadronic channels, and signals are identified using

$$M_{bc} = \sqrt{(E_{cm}/2)^2 - P_B^2}$$

$$\Delta E = E_B - E_{cm}/2$$

$$\Delta E' = \Delta E + M_{bc} - m_B$$

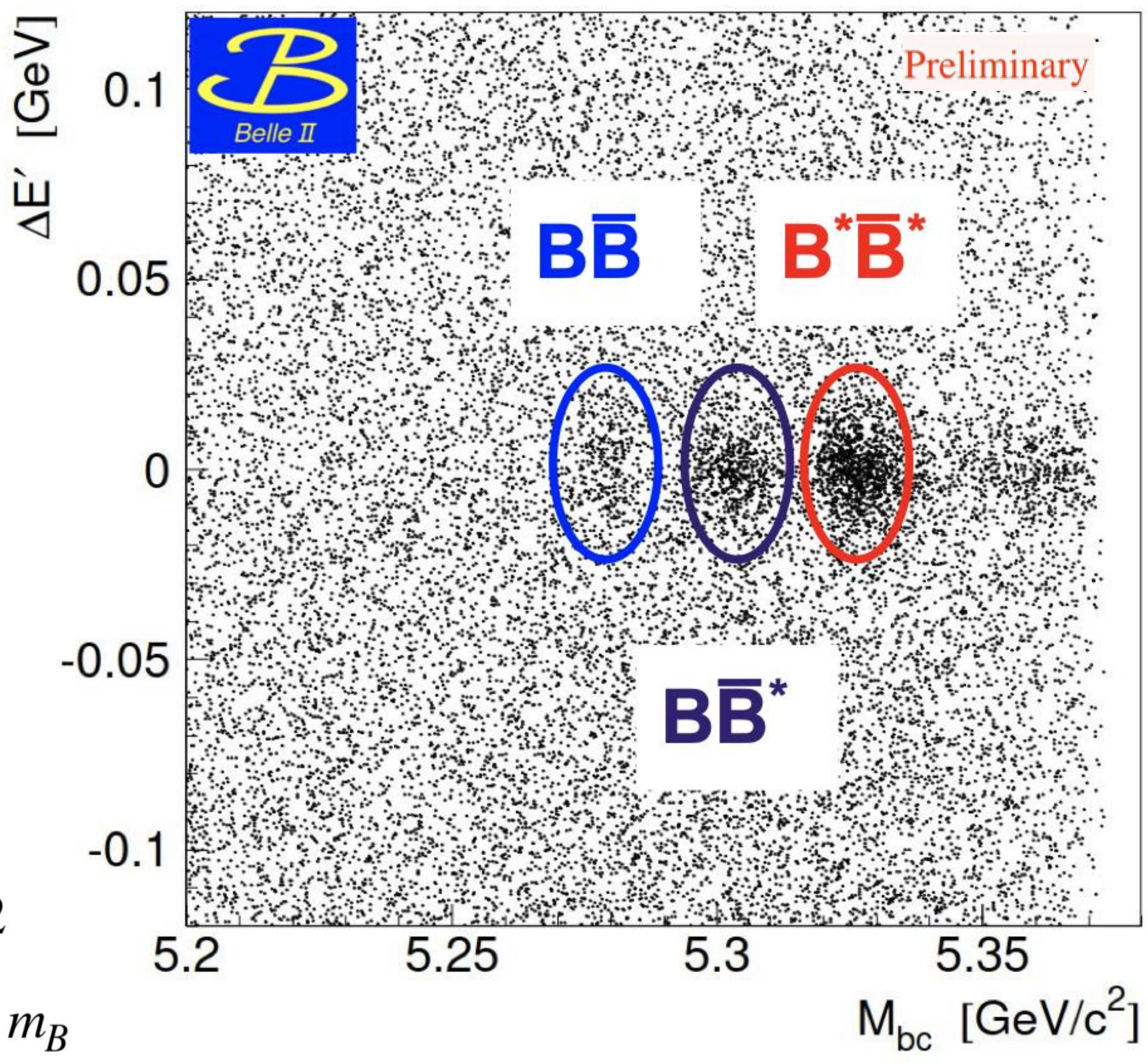

M_{bc} fit at scan energies

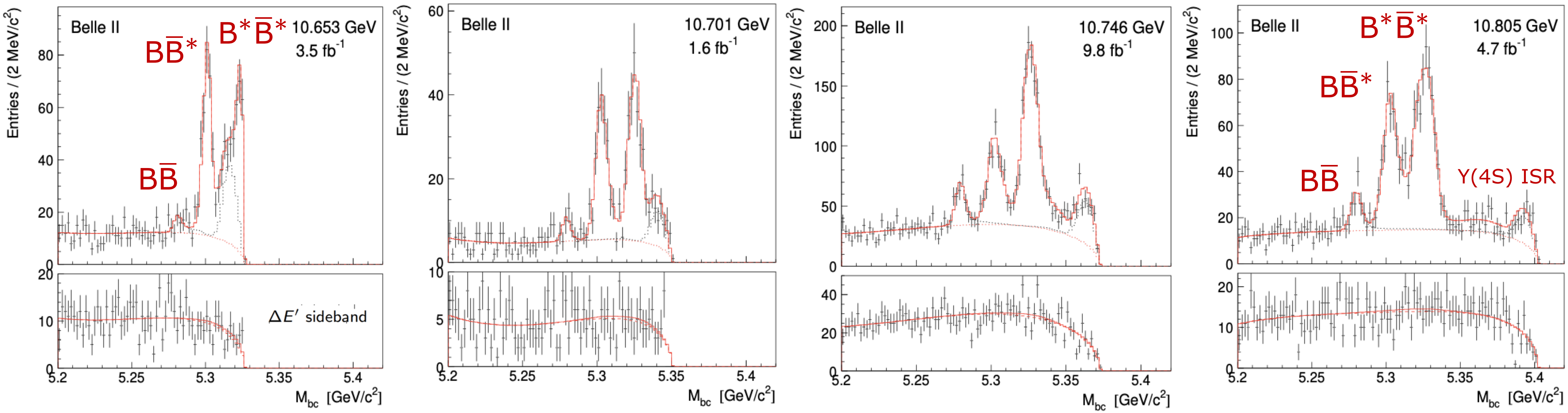

- $e^+e^- \to B\bar{B}$, $B\bar{B}^*$ and $B^*\bar{B}^*$ signals at $\sqrt{s} \sim 10.75$ GeV can be clearly observed
- Contribution of $\Upsilon(4S) \to B\bar{B}$ production via ISR is visible well (black dotted histograms)
- At $\sqrt{s}$ =10.653 GeV, the sharp cut of the data at right edge is due to threshold effect

Energy dependence of the cross sections

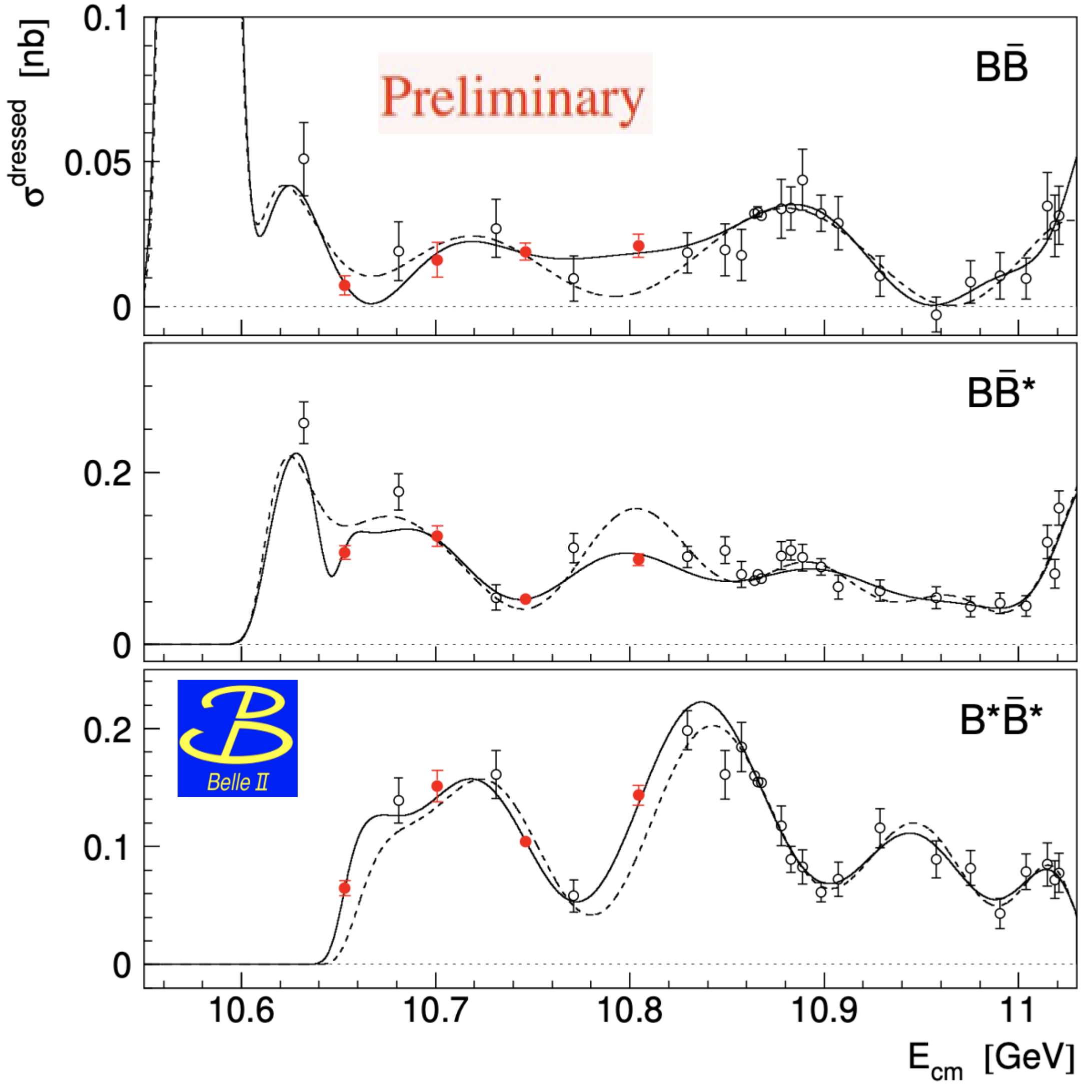

Solid curve – combined Belle + Belle II data fit
Dashed curve – Belle data fit only

New: rapid increase of $\sigma_{B^*\bar{B}^*}$ above the threshold

- Similar behaviour was seen for $D^*\bar{D}^*$ cross section (PRD 97, 012002 (2018))
- Possible interpretation: resonance or bound state ($B^*\bar{B}^*$ or $b\bar{b}$) near threshold (MPL A 21, 2779 (2006))
- Also explains a narrow dip in $\sigma(e^+e^- \to B\bar{B}^*)$ near $B^*\bar{B}^*$ threshold by destructive interference between $e^+e^- \to B\bar{B}^*$ and $e^+e^- \to B^*\bar{B}^* \to B\bar{B}^*$
- Inelastic channels [$\pi^+\pi^-\Upsilon(nS)$ and $h_b(1P)\eta$] could also be enhanced (PRD 87, 094033 (2013))

Search for $e^+e^- \to \omega\eta_b(1S)$ and $e^+e^- \to \omega\chi_{b0}(1P)$

- Tetraquark (diquark-antidiquark) interpretation of this state predicts enhancement of $\Upsilon(10753) \to \omega\eta_b(1S)$ transition [Chin. Phys. C 43, 123102 (2019)].

$$\frac{\Gamma(\eta_b\ \omega)}{\Gamma(\Upsilon\ \pi^+\pi^-)} \sim 30$$

- The $e^+e^- \to \omega\chi_{bJ}(1P)$ (J = 1, 2) was found to be enhanced at $\sqrt{s}$ = 10.745 GeV (PRL 130, 091902 (2023)). The $e^+e^- \to \omega\chi_{b0}(1P)$ transition was not observed due to low $\mathcal{B}[\chi_{b0}(1P) \to \gamma\Upsilon(1S)] = (1.94 \pm 0.27)\%$.

- We reconstruct only $\omega \to \pi^+\pi^-\pi^0$ and use its recoil mass to identify the signal.

$$M_{\text{recoil}}(\pi^+\pi^-\pi^0) = \sqrt{\left(\frac{E_{\text{c.m.}} - E^*}{c^2}\right)^2 - \left(\frac{p^*}{c}\right)^2}$$

Recoil mass spectra of $\pi^+\pi^-\pi^0$

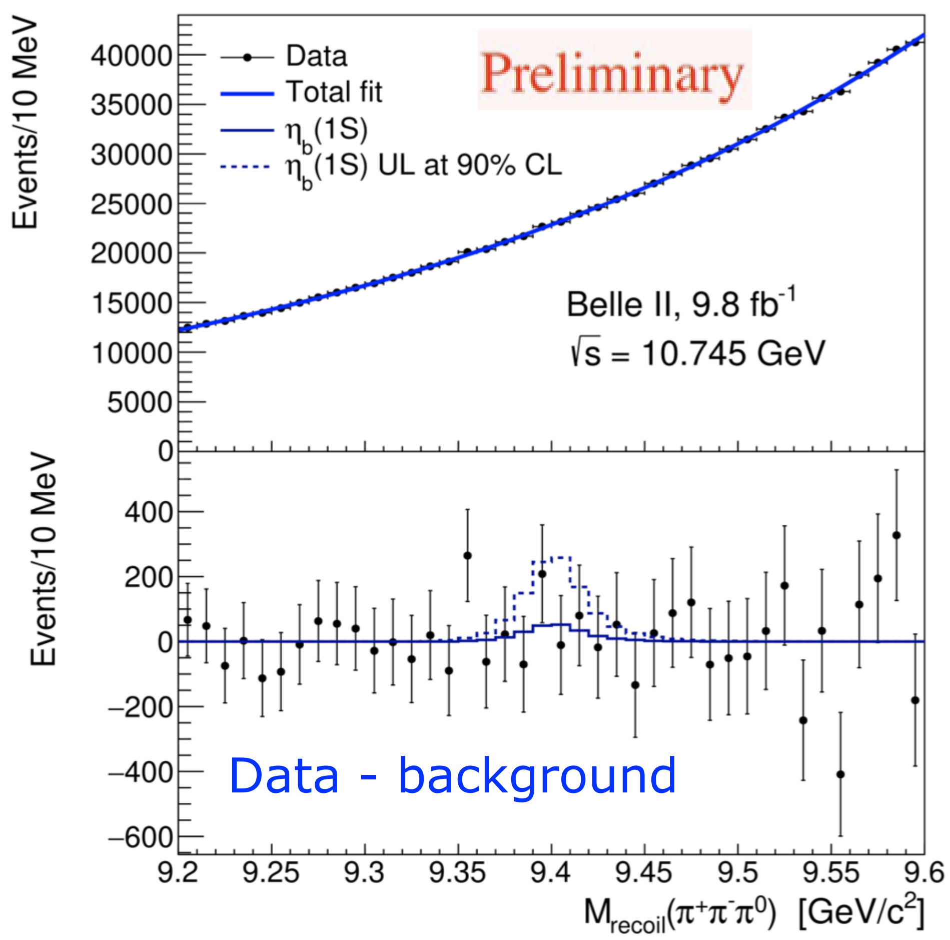

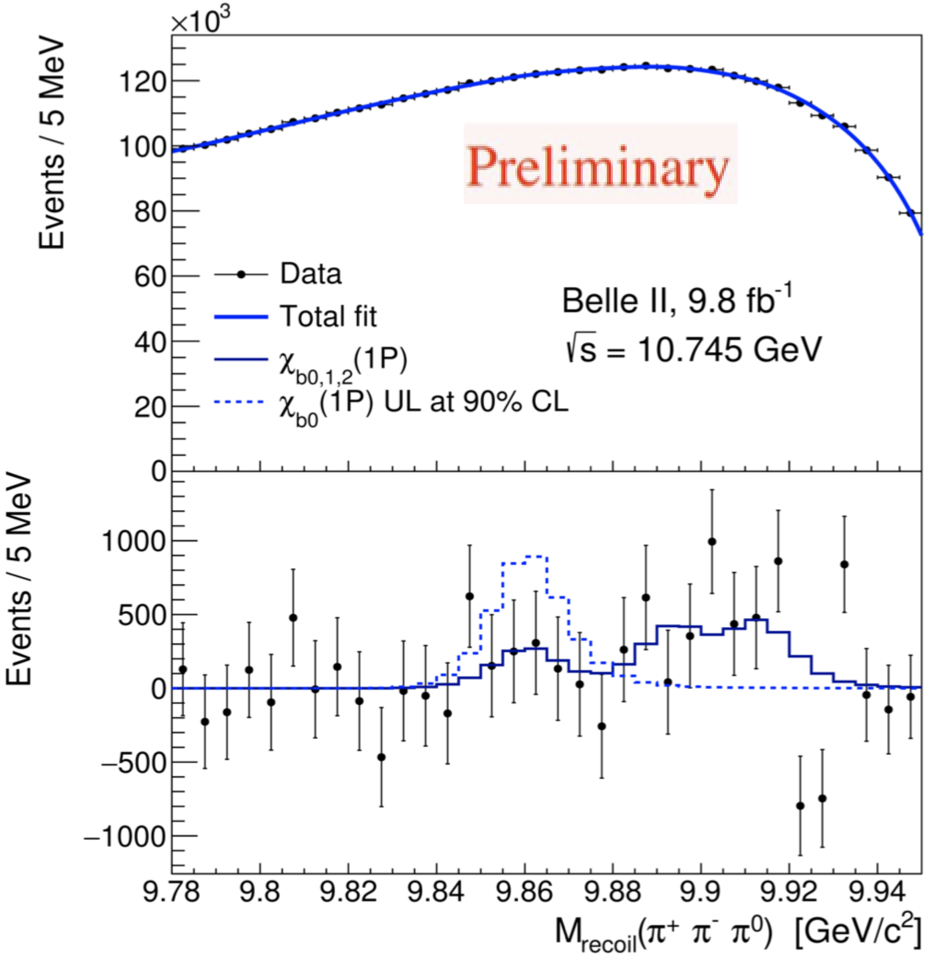

- A 3rd polynomial for $\eta_b(1S)$
- A product of a 4th polynomial and a square root function for $\chi_{b0}(1P)$
- Polynomial orders are chosen with maximum p-values

- The yields for $\chi_{b1}(1P)$ and $\chi_{b2}(1P)$ are fixed [PRL 130, 091902 (2023)].

Channel	$e^+e^- \to \eta_b(1S)\omega$	$e^+e^- \to \chi_{b0}(1P)\omega$
Yield	$(0.23 \pm 0.49 \pm 0.25) \cdot 10^3$	$(1.2 \pm 1.4 \pm 0.9) \cdot 10^3$

No clear $\eta_b(1S)$ and $\chi_{b0}(1P)$ signals are observed.

Born cross sections

Preliminary

$$\sigma_{\rm B}[e^+e^- \to X\omega] = \frac{N \cdot |1-\Pi|^2}{\varepsilon \cdot \mathcal{L} \cdot (1+\delta_{\rm ISR}) \cdot \mathcal{B}_{int}}$$

Channel	$e^+e^- \to \eta_b(1S)\omega$	$e^+e^- \to \chi_{b0}(1P)\omega$
Yield (10^3)	$0.23 \pm 0.49 \pm 0.25$	$1.2 \pm 1.4 \pm 0.9$
Born section section (pb)	$0.5 \pm 1.1 \pm 0.6$	$2.6 \pm 3.1 \pm 2.1$
Upper limit at 90% C.L. (pb)	<2.5	<8.7

Upper limits at the 90% CL are set using the Feldman-Cousins method [Phys. Rev. D 57, 3873 (1998)]

Tetraquark model in Ref. [CPC 43, 123102 (2019)]:

$$\Gamma(\Upsilon(10753) \to \eta_b(1S)\omega) = 2.64^{+4.70}_{-1.69}\ \mathrm{MeV}$$

$$\Gamma(\Upsilon(10753) \to \Upsilon\pi^+\pi^-) = 0.08^{+0.20}_{-0.06}\ \mathrm{MeV}$$

This measurement and JHEP 10, 220 (2019):

$$\sigma^B(\Upsilon(10753) \to \eta_b(1S)\omega) < 2.5\ \mathrm{pb}$$

$$\sigma^B(\Upsilon(10753) \to \Upsilon(2S)\pi^+\pi^-) \approx (3 \pm 1)\ \mathrm{pb}$$

Our results do not support the prediction within the tetraquark model that the $\Upsilon(10753) \to \omega\eta_b(1S)$ decay is enhanced.

Updated measurement of the energy dependence of the $e^+e^- \to \pi^+\pi^-\Upsilon(nS)$ cross sections

Preliminary

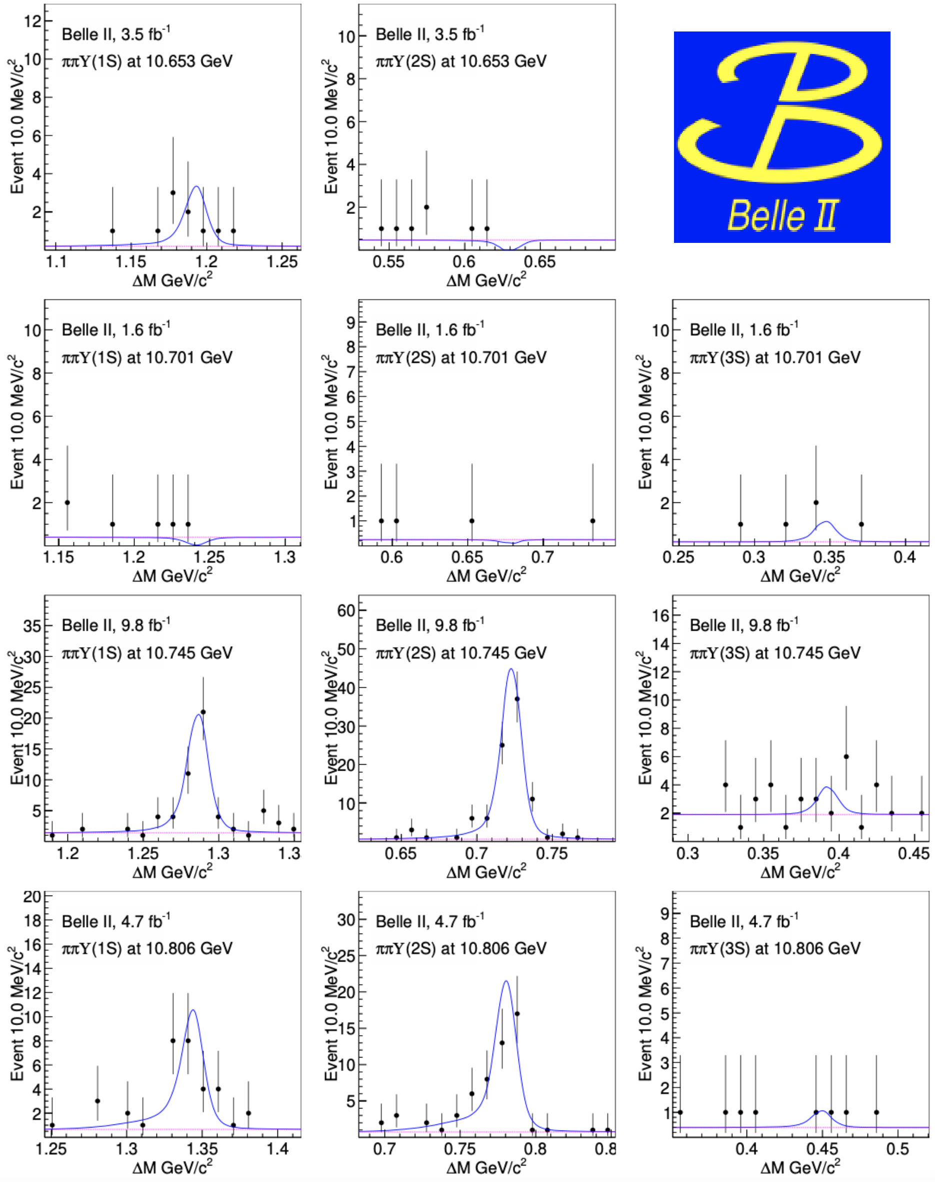

- $\Delta M = M(\pi^+\pi^-\mu^+\mu^-) - M(\mu^+\mu^-)$ is defined to extract the signal.
- Significant signals for $\Upsilon(1S, 2S)\pi^+\pi^-$ at $\sqrt{s} = 10.745,\ 10.806$ GeV
- No evident signals for $\Upsilon(3S)\pi^+\pi^-$
- Significance for $\Upsilon(1S)\pi^+\pi^-$ at $\sqrt{s} = 10.653$ GeV is only $1.7 \sim 2.3\sigma$, depending on different background assumptions.

Intermediate state —$M(\pi\pi)$

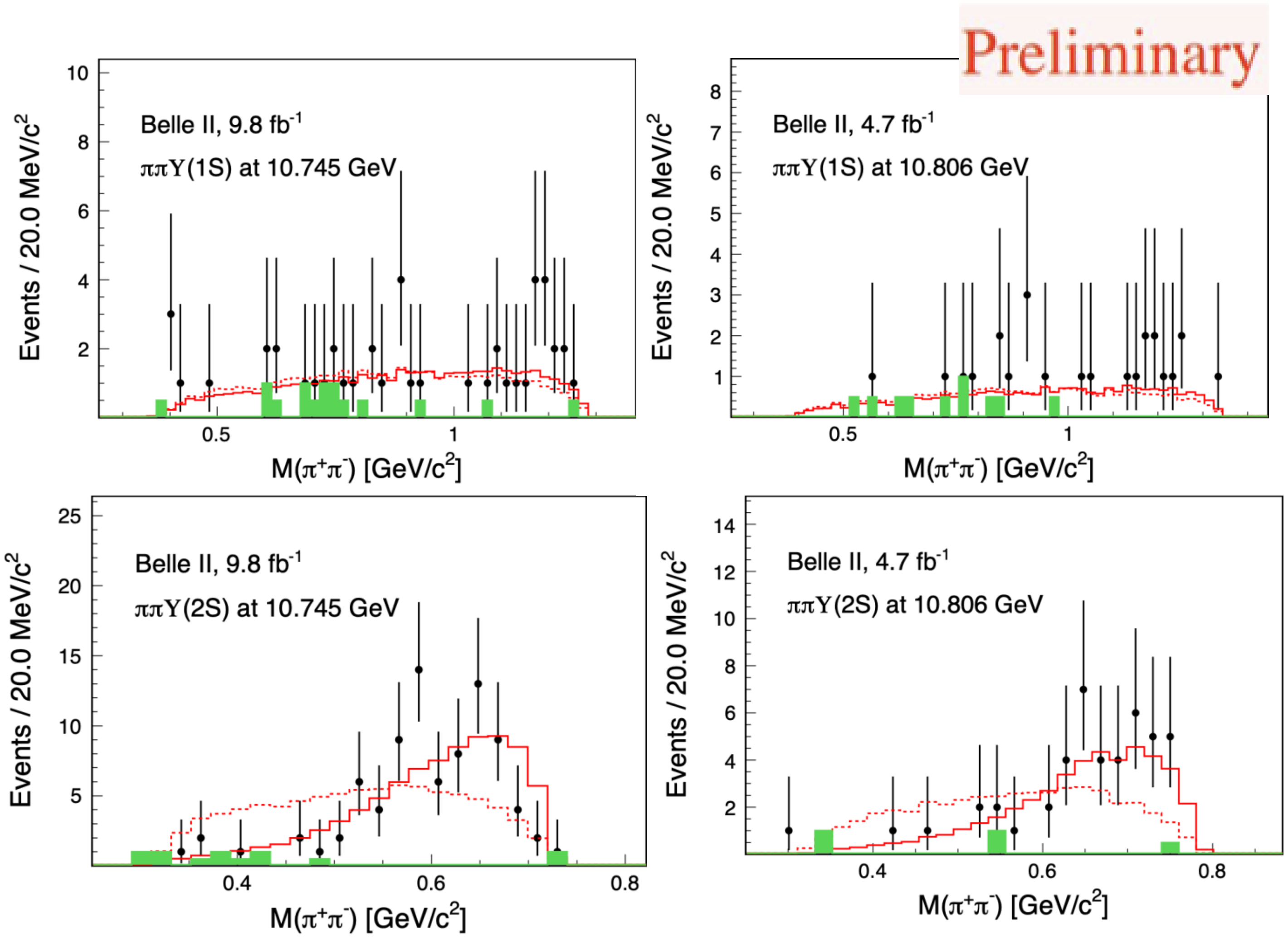

Dots: events in signal region

Green: nearest sidebands, scaled with area

Red dashed: signal MC, simulated uniformly

Red solid： re-weighted signal MC

$\Upsilon(1S)\pi\pi$ ：

Consistent with PHSP

$(\chi^2 = 0.98, 1.14\ )$

$\Upsilon(2S)\pi\pi$ ：

Not consistent with PHSP

$(\chi^2 = 3.45, 2.43)$

Intermediate state — $M_{\text{recoil}}(\pi)$

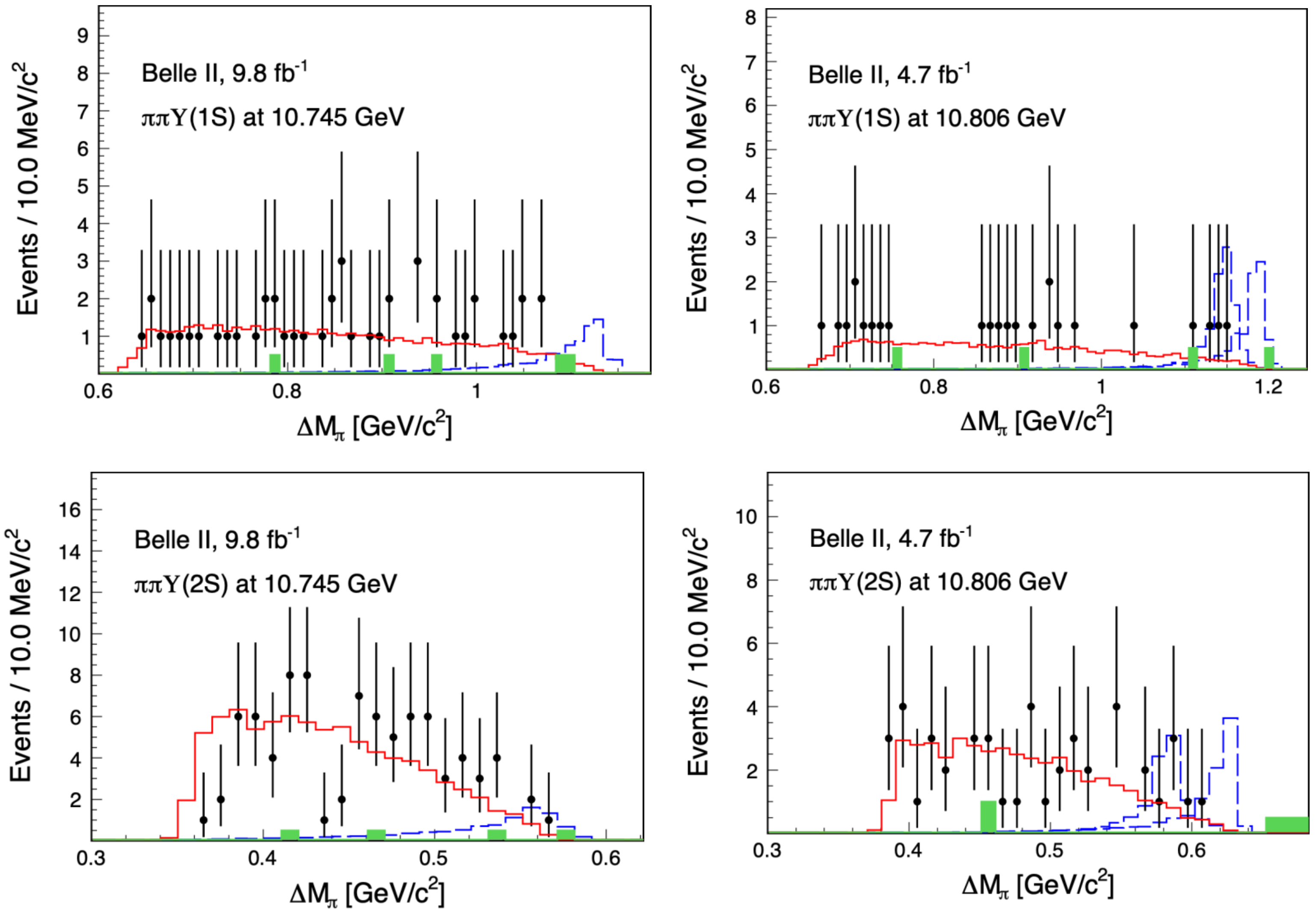

- No evidence of $Z_b(10610/10650)$.
- Upper limits estimated at 90% C.L.

Preliminary

	10.745 GeV		10.805 GeV	
Mode	$\pi\Upsilon(1S)$	$\pi\Upsilon(2S)$	$\pi\Upsilon(1S)$	$\pi\Upsilon(2S)$
$N_{\text{UL}}(Z_{b1})$	< 4.9	< 13.8	< 5.2	< 12.3
$N_{\text{UL}}(Z_{b2})$	–	–	< 5.8	< 6.0
ϵ_1	0.247	0.399	0.256	0.472
ϵ_2	–	–	0.395	0.270
$\sigma^B_{\text{UL}}(Z_{b1})$ (pb)	< 0.13	< 0.14	< 0.43	< 0.35
$\sigma^B_{\text{UL}}(Z_{b2})$ (pb)	–	–	< 0.28	< 0.30

Updated cross sections

Fit with three coherent BW, convoluting a Gaussian modeling energy spread:

$$\sigma \propto |\sum_i^3 \frac{\sqrt{12\pi\Gamma_i\mathcal{B}_i}}{s - M_i + iM_i\Gamma_i} \cdot \sqrt{\frac{f(\sqrt{s})}{f(M_i)}} e^{i\phi_i}|^2 \otimes G(0, \delta E)$$

All parameters are free, except $\delta E = 0.0056 \text{ GeV}$

Parameters of $\Upsilon(10753)$:

$M = 10756.3 \pm 2.7_{(stat.)} \pm 0.6_{(syst.)} \mathrm{MeV}/c^2$

$\Gamma = 29.7 \pm 8.5_{(stat.)} \pm 1.1_{(syst.)} \mathrm{MeV}$

Relative ratios of cross section at different resonance peaks

	$\mathcal{R}^{\Upsilon(10753)}_{\sigma(1S/2S)}$	$\mathcal{R}^{\Upsilon(10753)}_{\sigma(3S/2S)}$	$\mathcal{R}^{\Upsilon(5S)}_{\sigma(1S/2S)}$	$\mathcal{R}^{\Upsilon(5S)}_{\sigma(3S/2S)}$	$\mathcal{R}^{\Upsilon(6S)}_{\sigma(1S/2S)}$	$\mathcal{R}^{\Upsilon(6S)}_{\sigma(3S/2S)}$
Ratios	$0.46^{+0.15}_{-0.12}$	$0.10^{+0.05}_{-0.04}$	$0.45^{+0.04}_{-0.04}$	$0.32^{+0.04}_{-0.03}$	$0.64^{+0.23}_{-0.13}$	$0.41^{+0.16}_{-0.12}$

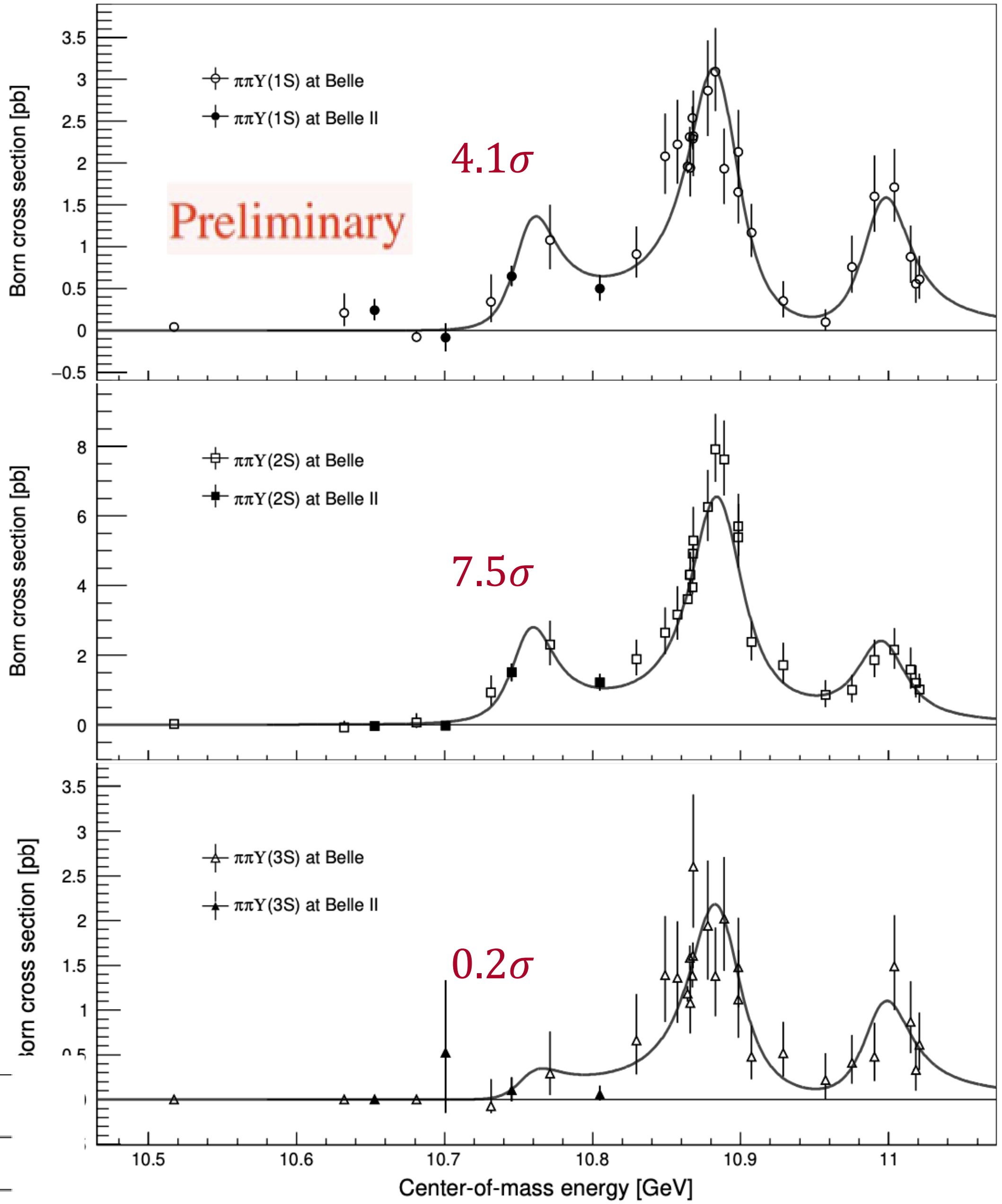

Measurements of $\Lambda_c^+ \to \Sigma^+\pi^0, \Sigma^+\eta$ and $\Sigma^+\eta'$

■ Motivation

PRD 107, 032003 (2023)

- For the charmed baryon weak decays: $B_c \to B + M$, there are six topological diagrams. Among them, T and C are factorizable, while C′ and E_{1-3} are nonfactorizable.
- All the nonfactorizable diagrams contribute to $\Lambda_c^+ \to \Sigma^+\eta(\eta')$.

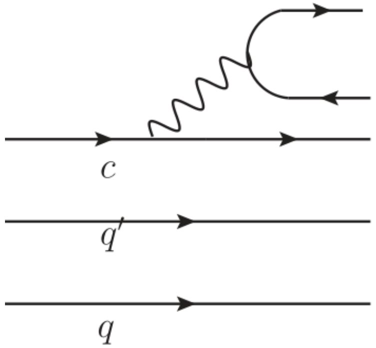

T

external W-emission T

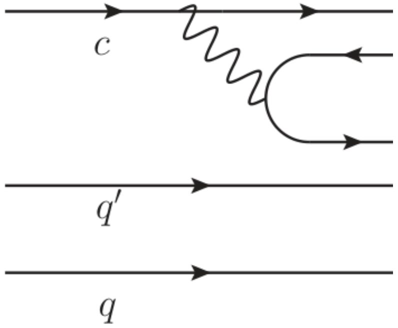

C

internal W-emission C

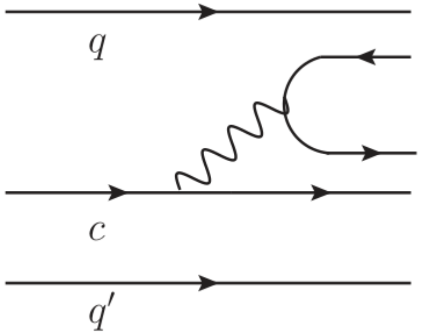

C'

inner W-emission C'

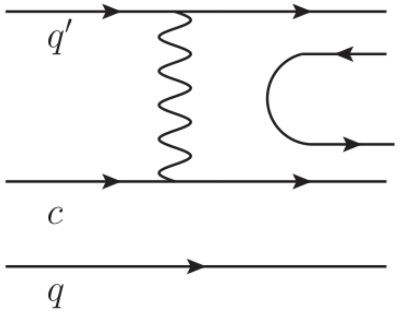

E_1

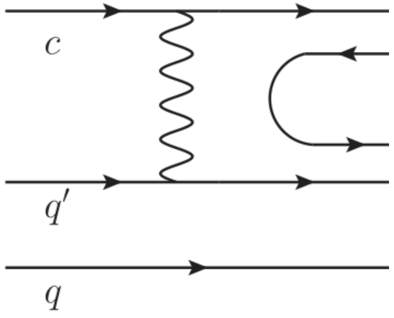

E_2

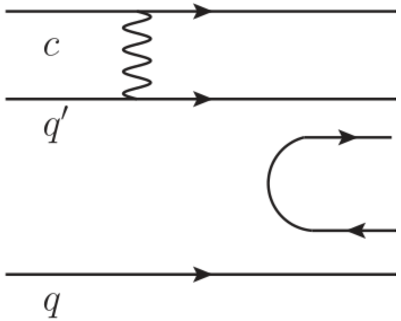

E_3

W-exchange diagrams E_1 E_2 E_3

Measurements of $\Lambda_c^+ \to \Sigma^+\pi^0, \Sigma^+\eta$ and $\Sigma^+\eta'$

Motivation

PRD 107, 032003 (2023)

- Theoretical predictions on the branching fractions and asymmetry parameters of $\Lambda_c^+ \to \Sigma^+\eta(\eta')$ vary across.

- Branching fractions of $\Lambda_c^+ \to \Sigma^+\eta(\eta')$ are measured with large uncertainty (δB/B>40%) [PDG]. Decay asymmetry parameters for these two modes have never been measured.

Decay	Körner CCQM	Xu Pole	Cheng CA	Cheng Pole	Ivanov CCQM	Żenczykowski Pole	Sharma CA	Zou CA	Geng SU(3)	Experiment
$\Lambda_c^+ \to \Sigma^+\eta$	0.16				0.11	0.90	0.57	0.74	0.32 ± 0.13	0.44 ± 0.20
$\Lambda_c^+ \to \Sigma^+\eta'$	1.28				0.12	0.11	0.10		1.44 ± 0.56	1.5 ± 0.6
$\Lambda_c^+ \to \Sigma^+\eta$	0.33				0.55	0	-0.91	-0.95	-0.40 ± 0.47	
$\Lambda_c^+ \to \Sigma^+\eta'$	-0.45				-0.05	-0.91	0.78		$1.00^{+0.00}_{-0.17}$	

Branching fractions

Asymmetry parameters

Measurements of $\Lambda_c^+ \to \Sigma^+\pi^0, \Sigma^+\eta$ and $\Sigma^+\eta'$

- **Measurements of branching fractions of $\Lambda_c^+ \to \Sigma^+\eta$ and $\Lambda_c^+ \to \Sigma^+\eta'$** $(\Sigma^+ \to p\pi^0;\ \eta' \to \eta\pi\pi; \eta \to \gamma\gamma)$

full Belle datasets

Method: $$\frac{B(\Lambda_c^+ \to \Sigma^+\eta/\Sigma^+\eta')}{B(\Lambda_c^+ \to \Sigma^+\pi^0)} = \frac{y(\Lambda_c^+ \to \Sigma^+\eta/\Sigma^+\eta')}{B_{\mathrm{PDG}} \times y(\Lambda_c^+ \to \Sigma^+\pi^0)}$$ (y is the efficiency-corrected yield).

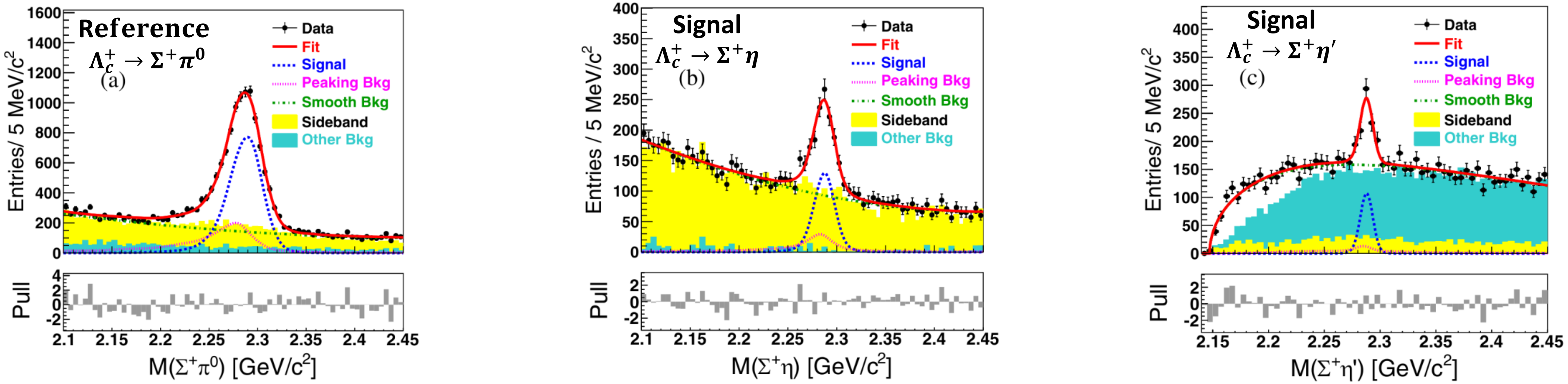

$$\frac{B(\Lambda_c^+ \to \Sigma^+\eta)}{B(\Lambda_c^+ \to \Sigma^+\pi^0)} = 0.25 \pm 0.03 \pm 0.01; \quad B(\Lambda_c^+ \to \Sigma^+\eta) = (3.14 \pm 0.35 \pm 0.11 \pm 0.25) \times 10^{-3}$$

$$\frac{B(\Lambda_c^+ \to \Sigma^+\eta')}{B(\Lambda_c^+ \to \Sigma^+\pi^0)} = 0.33 \pm 0.06 \pm 0.02; \quad B(\Lambda_c^+ \to \Sigma^+\eta') = (4.16 \pm 0.75 \pm 0.21 \pm 0.33) \times 10^{-3}$$

statistical   systematical   from $B(\Lambda_c^+ \to \Sigma^+\pi^0)$

PDG: $B(\Lambda_c^+ \to \Sigma^+\eta) = (4.4 \pm 2.0) \times 10^{-3}$

PDG: $B(\Lambda_c^+ \to \Sigma^+\eta') = (15 \pm 6) \times 10^{-3}$

Consistent with PDG. Most precise result to date

Measurements of $\Lambda_c^+ \to \Sigma^+\pi^0, \Sigma^+\eta$ and $\Sigma^+\eta'$

■ **Measurements of asymmetry parameters of $\Lambda_c^+ \to \Sigma^+\pi^0,\ \Sigma^+\eta,$ and $\Sigma^+\eta'$**

The differential decay rate depends on the asymmetry parameter α_{Σ^+X} as:

$$\frac{dN}{dcos\theta_{\Sigma^+}} \propto 1 + \alpha_{\Sigma^+X}\alpha_{p\pi^0}cos\theta_{\Sigma^+}$$

$\alpha_{p\pi^0} = -0.982 \pm 0.014$ from world average value.

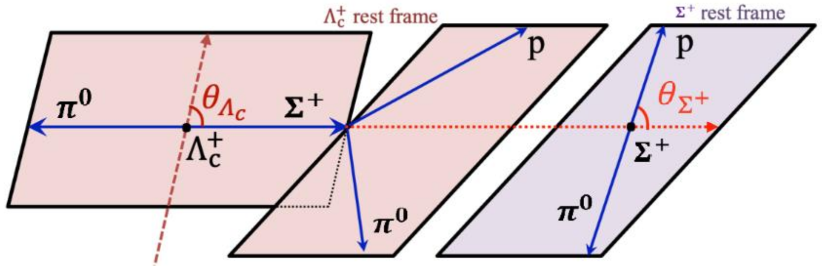

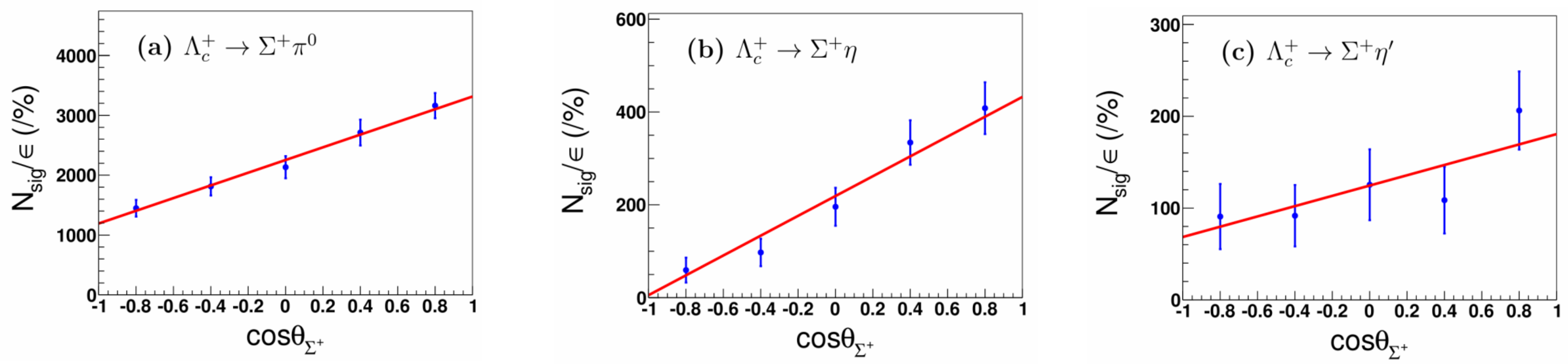

- $\alpha_{\Sigma^+\pi^0} = -0.48 \pm 0.02 \pm 0.02$
  - agrees with the world average value: -0.55 ± 0.11.
  - with much improved precision.
  - The consistency with $\alpha_{\Sigma^0\pi^+} = -0.463 \pm 0.016 \pm 0.008$ indicates no isospin symmetry broken.
- $\alpha_{\Sigma^+\eta} = -0.99 \pm 0.03 \pm 0.05$ and $\alpha_{\Sigma^+\eta'} = -0.46 \pm 0.06 \pm 0.03$
  - measured for the first time.

Branching fractions of $\Lambda_c^+ \to pK_S^0K_S^0, pK_S^0\eta$

Motivation

PRD 107, 032004 (2023)

- Precise measurements of branching fractions of charmed baryon weak decays are useful for studying the dynamics of charmed baryons and testing the predictions of theoretical models.

- No result of branching fraction for $\Lambda_c^+ \to pK_S^0K_S^0$ is reported. According to theoretically results based on SU(3)F symmetry [EPJC 79 (2019) 946], we estimate $\sim O(10^3)$ signal yield at Belle.

- Measured branching fraction $\mathrm{B}(\Lambda_c^+ \to pK_S^0\eta) = (4.15 \pm 0.90) \times 10^{-3}$ has large uncertainty (δB/B~20%) [PDG]. We target at an improved precision of BF.

- Check Dalitz-plot for the intermediate resonances existence, e.g. N*(1535).

Branching fractions of $\Lambda_c^+ \to pK_S^0K_S^0, pK_S^0\eta$

full Belle datasets

Signal Yield Extraction

Signal: $\Lambda_c^+ \to pK_S^0K_S^0$ **Signal: $\Lambda_c^+ \to pK_S^0\eta$** **Reference: $\Lambda_c^+ \to pK_S^0$**

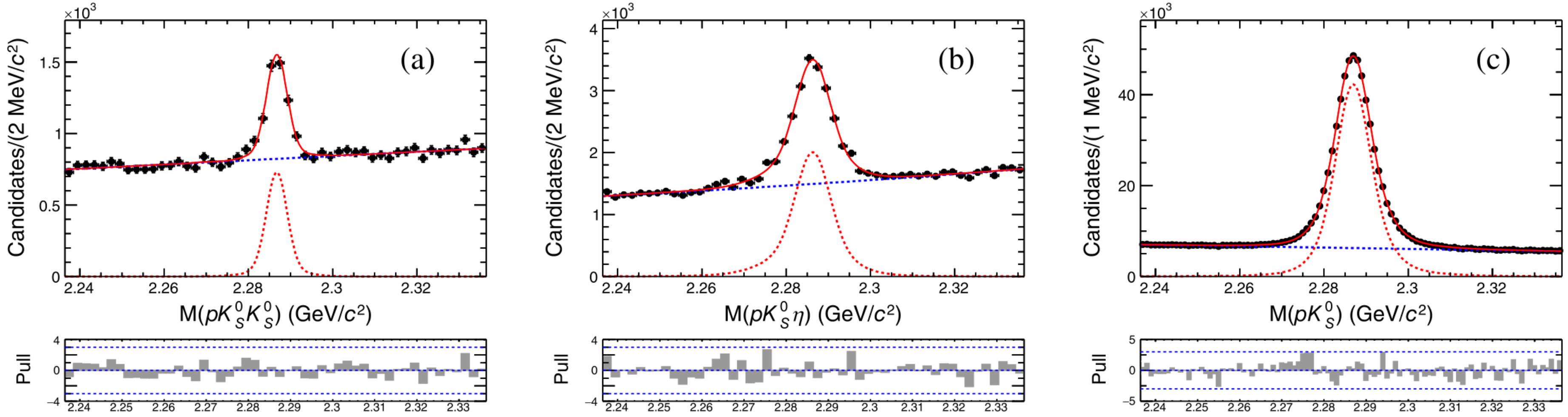

Yields	$\Lambda_c^+ \to pK_S^0K_S^0$	$\Lambda_c^+ \to pK_S^0\eta$	$\Lambda_c^+ \to pK_S^0$
$N_{\rm sig}^{\rm FR}$	2442 ± 103	12877 ± 317	515296 ± 1129

Efficiency Plane

- For reference mode, directly use the efficiency from MC.
- For signal modes, possible intermediate structures affect on final averaged efficiencies. Therefore, we use the Dalitz-plot-based efficiency planes.

Branching fractions of $\Lambda_c^+ \to pK_S^0K_S^0, pK_S^0\eta$

Efficiency Plane

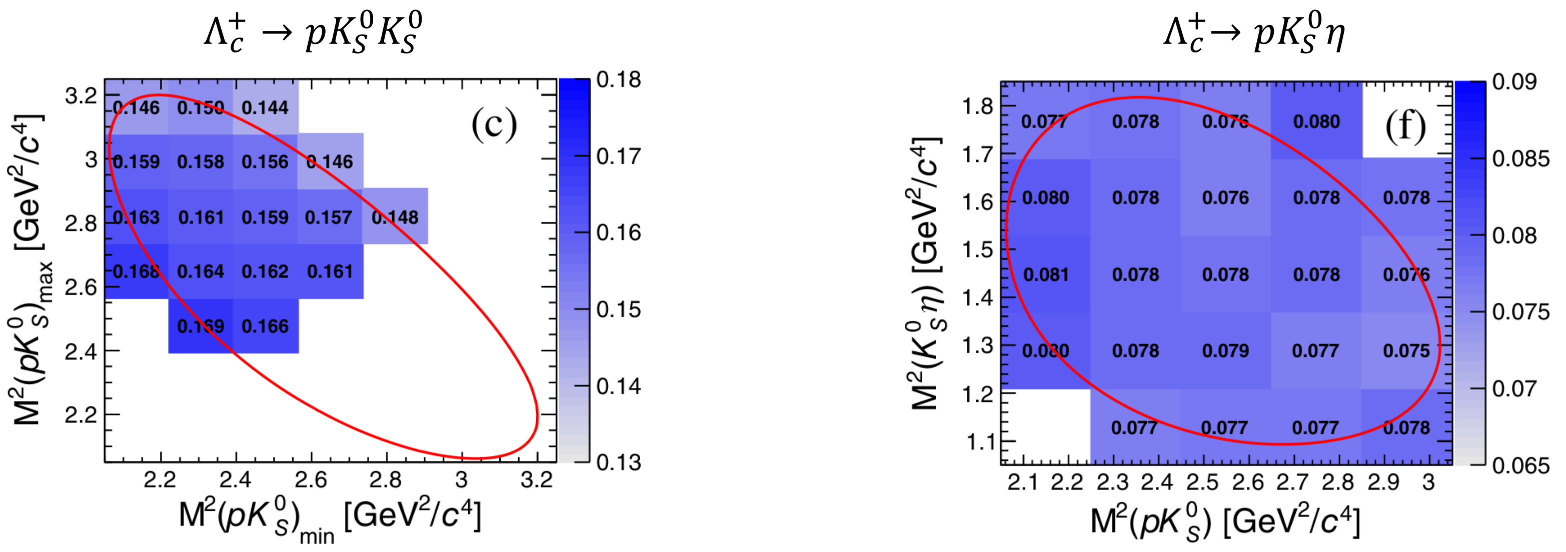

Plots (c, f) show the average signal efficiency in bins across the Dalitz plane. The red curves show the edges of kinematic phase-space region of the decays.

Branching fraction

$$\frac{B(\Lambda_c^+ \to pK_S^0K_S^0, pK_S^0\eta)}{B(\Lambda_c^+ \to pK_S^0)} = \frac{y(\Lambda_c^+ \to pK_S^0K_S^0, pK_S^0\eta)}{B_{\text{PDG}} \times y(\Lambda_c^+ \to pK_S^0)}$$

(y is the efficiency-corrected yield).

- $\frac{B(\Lambda_c^+ \to pK_S^0K_S^0)}{B(\Lambda_c^+ \to pK_S^0)} = (1.48 \pm 0.08 \pm 0.04) \times 10^{-2}$ ➡ $B(\Lambda_c^+ \to pK_S^0K_S^0) = (2.35 \pm 0.12 \pm 0.07 \pm 0.12) \times 10^{-4}$
  - ➢ First observation
- $\frac{B(\Lambda_c^+ \to pK_S^0\eta)}{B(\Lambda_c^+ \to pK_S^0)} = (2.73 \pm 0.06 \pm 0.13) \times 10^{-1}$ ➡ $B(\Lambda_c^+ \to pK_S^0\eta) = (4.35 \pm 0.10 \pm 0.20 \pm 0.22) \times 10^{-3}$
  - ➢ Consistent with world average value $(4.15 \pm 0.90) \times 10^{-3}$ and threefold improvement in precision.

Search for the semileptonic decays of $\Xi_c^0 \to \Xi^0 \ell^+ \ell^-$ at Belle

Motivation

- Experimental study of baryonic semileptonic decays can test the Lepton Flavor University (LFU) and provide important inputs for theoretical studies.
- Few neutrino-less decays were observed experimentally[1-4].
- Only upper limits were set for $\Lambda_c \to p\ell^+\ell^-$ decay for the charmed baryons[5,6].
- Both W-exchange and FCNC process contribute to $\Lambda_c \to p\ell^+\ell^-$, while some anomalies were reported for FCNC processes in B meson decays.
- The study of $\Xi_c^0 \to \Xi^0\ell^+\ell^-$ decays, related with $\Lambda_c \to p\ell^+\ell^-$ under SU(3) flavor symmetry [PRD 103, 013007(2021)], have not been measured experimentally.
- It will help the understanding of the charmed baryonic semileptonic decays, and allows an LFU test.

decays	Experimental results on $\mathcal{B}_f$	Ref.
$\Xi^0 \to \Lambda e^+ e^-$	$(7.6 \pm 0.4 \pm 0.4 \pm 0.2) \times 10^{-6}$	[1]PLB 650,1(2007)
$\Sigma^+ \to p\mu^+\mu^-$	$(8.6^{+6.6}_{-5.4} \pm 5.5) \times 10^{-8}$	[2]PRL 94,021801(2005)
$\Lambda_b \to \Lambda\mu^+\mu^-$	$(1.73 \pm 0.42 \pm 0.55) \times 10^{-6}$	[3]PRL 107,201802(2011)
$\Lambda_b \to \Lambda\mu^+\mu^-$	$(0.96 \pm 0.16 \pm 0.13 \pm 0.21) \times 10^{-6}$	[4]JHEP 06,115(2015)
$\Lambda_c \to pe^+e^-$	$< 5.5 \times 10^{-6}$ @ 90% C. L.	[5]PRD 84,072006(2011)
$\Lambda_c \to pe^+e^-$	$< 44 \times 10^{-6}$ @ 90% C. L.	[5]PRD 84,072006(2011)
$\Lambda_c \to p\mu^+\mu^-$	$< 7.7 \times 10^{-8}$ @ 90% C. L.	[6]PRD 97,091101(2018)

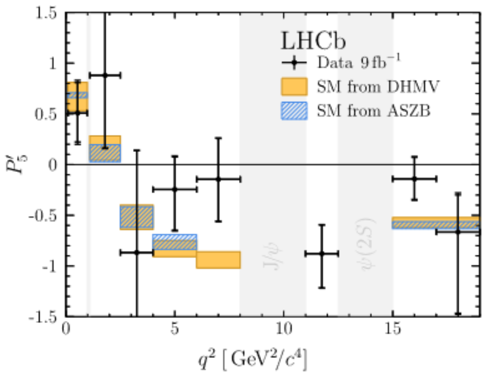

[7]PRL 126,161802(2021)

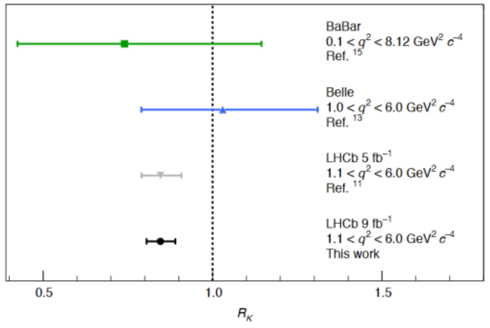

[8]Nat. Phys. 18, 277(2022)

Search for the semileptonic decays of $\Xi_c^0 \to \Xi^0 \ell^+ \ell^-$ at Belle

Overview

- Signal Ξ_c^0 MC samples are generated in $e^+e^- \to c\bar{c}$ process.
- Using full $\sim 1ab^{-1}$ Belle data, we directly reconstruct the $\Xi_c^0 \to \Xi^0 \ell^+ \ell^-$ decays.

Ξ^0 reconstruction

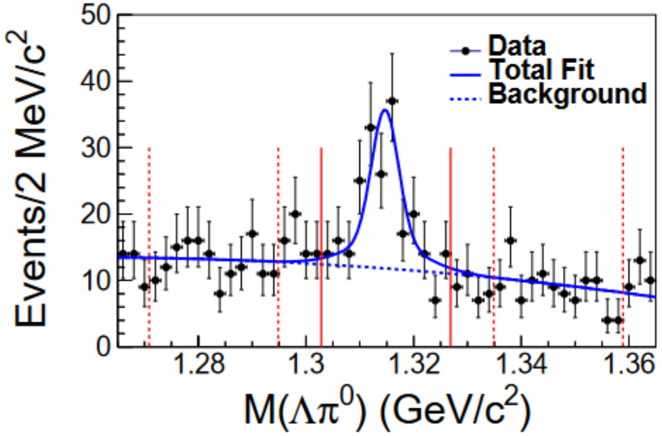

$\Xi^0 \ell^+ \ell^-$ invariant-mass spectra for (a) $\ell = e$ and (b) $\ell = \mu$.

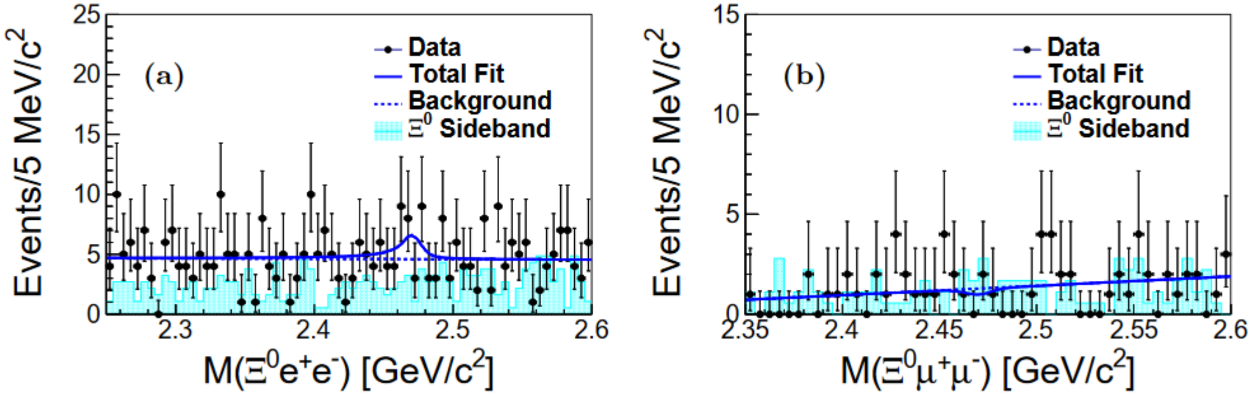

Results

- No significant signals are observed for the $\Xi^0 \ell^+ \ell^-$ invariant-mass spectra.
- 90% credibility upper limits on branching fractions are set:
  - $\mathcal{B}(\Xi_c^0 \to \Xi^0 \ell^+ \ell^-)/\mathcal{B}(\Xi_c^0 \to \Xi^- \pi^+) < 6.7\ (4.3) \times 10^{-3}$ and
  - $\mathcal{B}(\Xi_c^0 \to \Xi^0 \ell^+ \ell^-) < 9.9\ (6.5) \times 10^{-5}$ for electron (muon) mode.
- This analysis is to be submitted to Phys. Rev. D.

Mass and width of $\Lambda_c(2625)^+$ and BR of $\Lambda_c(2625)^+ \to \Sigma_c^{0,++}\pi$

Motivation

PRD 107, 032008 (2023)

- $\Lambda_c(2625)^+(J^P = 3/2^-)$ is the excited state of Λ_c^+. It dominantly decays to $\Lambda_c^+\pi^+\pi^-$ via P-wave decay. The D-wave decay $\Lambda_c(2625)^+ \to \Sigma_c^{0,++}\pi$ is also allowed, but its contribution is known to be small.

- The limited decay phase space of $\Lambda_c(2625)^+ \to \Lambda_c^+\pi^+\pi^-$ makes it difficult to extract the $\Sigma_c^{0,++}$ yields by fitting the $M(\Lambda_c^+\pi^\pm)$, due to the presence of reflection peaks formed by the combination of the Λ_c^+ and the other final-state pion. This can be solved by using a full Dalitz fit [PRD 98, 114007 (2018)].

- The mass of the $\Lambda_c(2625)^+$, relative to the Λ_c^+ mass, is already relatively well known [PRD 84,012003 (2011)], but the large Belle data sample allows for a more precise measurement.

- No intrinsic width of the $\Lambda_c(2625)^+$ has yet been measured, and the current upper limit $\Gamma < 0.97\ \mathrm{MeV}/c^2$ at 90% confidence level is based on the CDF measurement in 2011 [PRD 84,012003 (2011)].

Mass and width of $\Lambda_c(2625)^+$ and BR of $\Lambda_c(2625)^+ \to \Sigma_c^{0,++}\pi$

full Belle datasets

Measurements of mass and width

Reconstruction mode: $\Lambda_c(2625)^+ \to \Lambda_c^+\pi^+\pi^-, \Lambda_c^+ \to pK^-\pi^+$

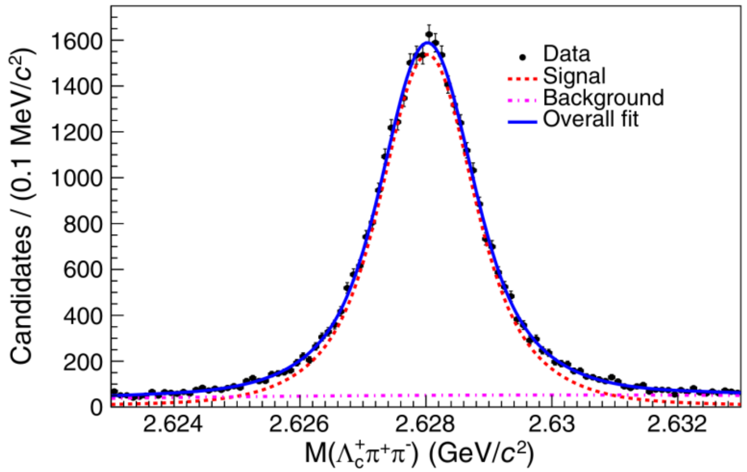

Fig: $M(\Lambda_c^+\pi^+\pi^-)$ distribution from data and corresponding fit result.

- $M[\Lambda_c(2625)^+] - M(\Lambda_c^+) = 341.518 \pm 0.006 \pm 0.049$ MeV/c^2
  - consistent with the world average value 341.65 ± 0.13 MeV/ c^2
  - has approximately half the uncertainty
- $\Gamma[\Lambda_c(2625)^+] < 0.52$ MeV
  - a factor of 2 more stringent than the previous limit $\Gamma < 0.97$ MeV
  - An improved limit on the width of the $\Lambda_c(2625)^+$ will help to constrain various theoretical predictions.

Mass and width of $\Lambda_c(2625)^+$ and BR of $\Lambda_c(2625)^+ \to \Sigma_c^{0,++}\pi$

Measurements of branching fractions

Full Dalitz plot fitted with AmpTools is performed [PRD 98, 114007 (2018)].

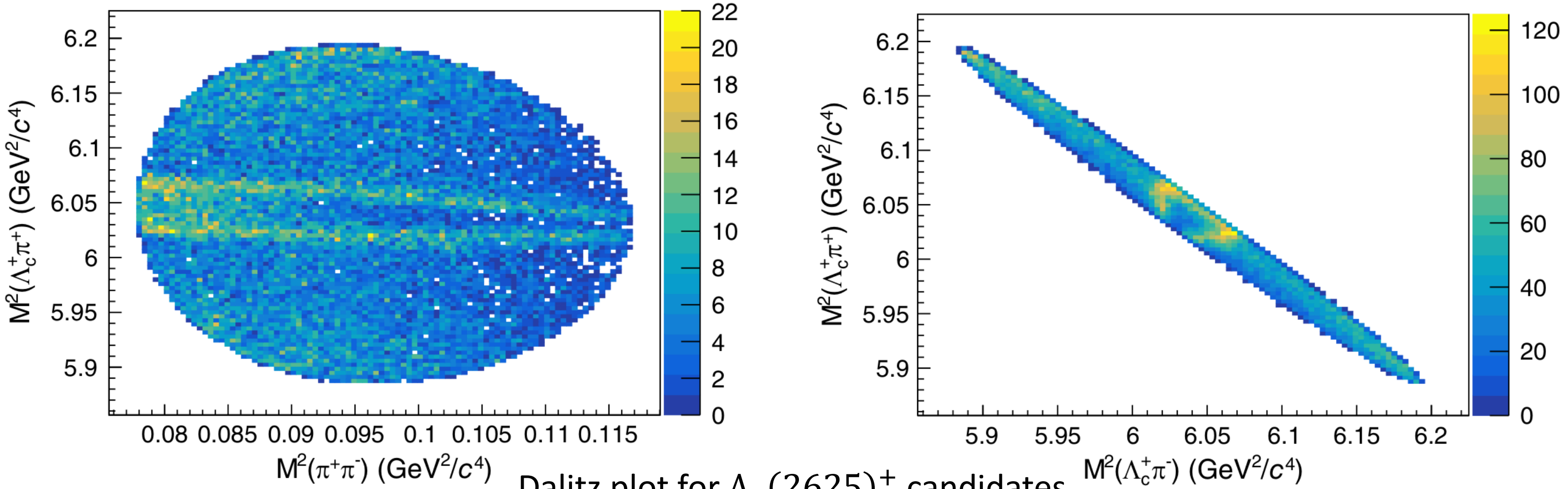

Dalitz plot for $\Lambda_c(2625)^+$ candidates

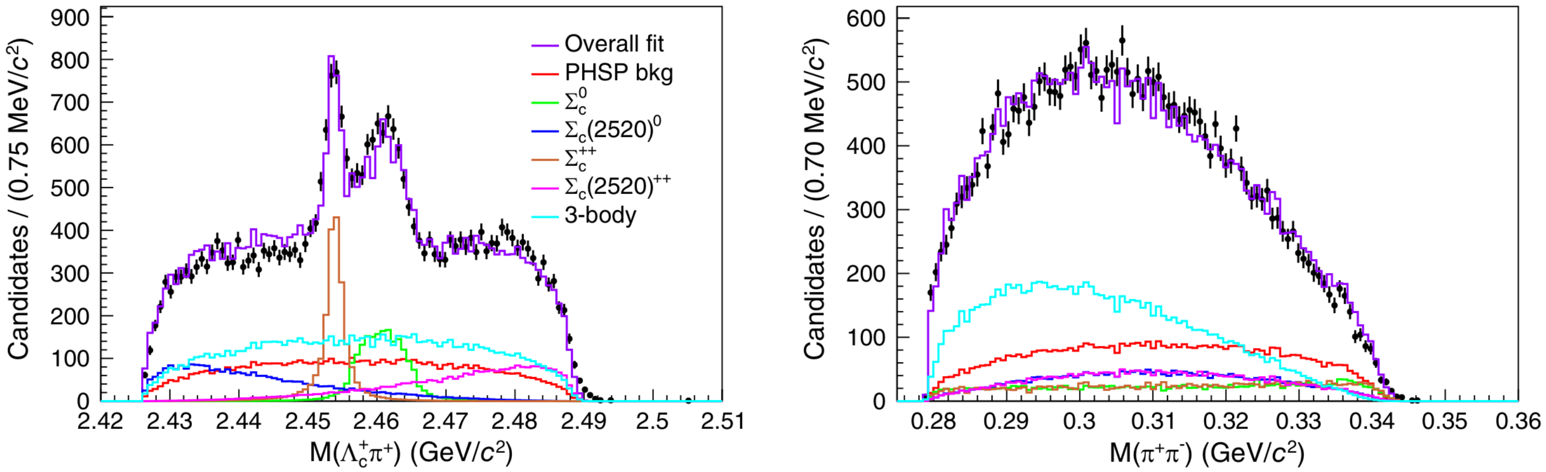

Dalitz plot fit result plotted as projections. Solid lines show the overall fitted distribution and its individual components as indicated in the legend.

Mass and width of $\Lambda_c(2625)^+$ and BR of $\Lambda_c(2625)^+ \to \Sigma_c^{0,++}\pi$

Measurements of branching fractions

The branching ratio of $\Lambda_c(2625)^+ \to \Sigma_c^{0,++}\pi$ relative to the reference mode $\Lambda_c(2625)^+ \to \Lambda_c^+\pi^+\pi^-$ is calculated by:

$$\frac{B(\Lambda_c(2625)^+ \to \Sigma_c^{0,++}\pi)}{B(\Lambda_c(2625)^+ \to \Lambda_c^+\pi^+\pi^-)} = \frac{y_{sig}(\Sigma_c^{0,++}) - y_{bkg}(\Sigma_c^{0,++})}{y_{sig}(\Lambda_c(2625)^+)}$$

(y is efficiency-corrected yield)

$y_{bkg}(\Sigma_c^{0,++})$ is obtained from sidebands of $\mathrm{M}(\Lambda_c^+\pi^+\pi^-)$. We obtain:

$$\frac{B(\Lambda_c(2625)^+ \to \Sigma_c^{0}\pi)}{B(\Lambda_c(2625)^+ \to \Lambda_c^+\pi^+\pi^-)} = (5.19 \pm 0.23 \pm 0.40)\%$$

$$\frac{B(\Lambda_c(2625)^+ \to \Sigma_c^{++}\pi)}{B(\Lambda_c(2625)^+ \to \Lambda_c^+\pi^+\pi^-)} = (5.13 \pm 0.26 \pm 0.32)\%$$

- The measured branching fraction ratios agree with PDG values and are the most precise to date.
- Our measurements align with the prediction that assuming $\Lambda_c(2625)^+$ is a λ mode excitation [PRD 98, 114007 (2018)].

$BR(B^+ \to K^+\nu\overline{\nu})$ in the Standard Model

The decay $B^+ \to K^+\nu\overline{\nu}$ occurs through a flavor-changing neutral current

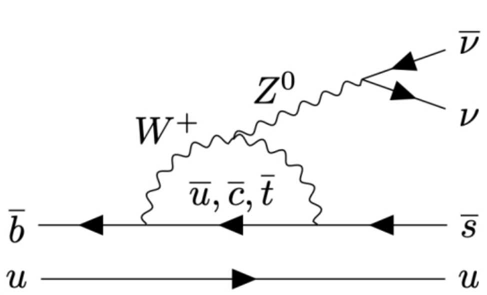

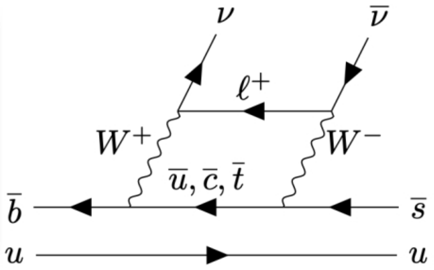

$$\mathscr{B}(B^+ \to K^+\nu\overline{\nu}) = (5.58 \pm 0.37) \times 10^{-6}$$

Phys. Rev. D 107, 1324 014511 (2023), arXiv:2207.13371 [hep-ph],
Phys. Rev. D 107, 119903 (2023)

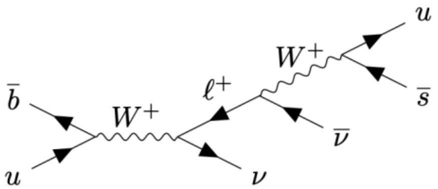

long-distance double-charged-current

- **Rare:** $b \to s\nu\overline{\nu}$ transition suppressed by the GIM mechanism
- **Precise SM prediction:** it does not suffer from hadronic uncertainties (beyond the form factors)

$BR(B^+ \to K^+\nu\bar{\nu})$ beyond the Standard Model

$\mathscr{B}(B^+ \to K^+\nu\bar{\nu})$ can be significantly modified in models that predict non-SM particles, such as leptoquarks:

PhysRevD.98.055003

JHEP09(2017)040

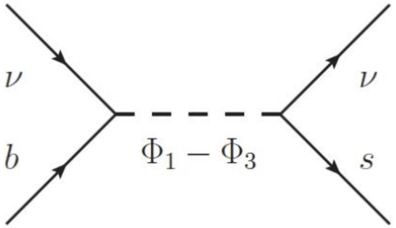

Indirect way to investigate the presence of multi-TeV particles

SM extensions predict $B^+ \to K^+X_{inv}$, where X_{inv} is an undetectable particle

X_{inv} could be a feebly interacting, long-lived, particle that escapes the detector (e.g., dark sector mediator) or a dark matter candidate.
Can be a scalar as in models with dark sector mixing with the SM Higgs PhysRevD.101.095006 or a pseudo-scalar such as an axion or axion-like-particle PhysRevD.102.015023, JHEP03(2015)171

Experimental status

No evidence for a signal observed to date Current best experimental upper limit: 1.6×10^{-5} at 90 % CL
PhysRevD.87.112005 [BaBar]

The first analysis on $B^+ \to K^+ \nu\bar{\nu}$ performed by Belle II used a limited dataset: L = 63 fb^{-1}

- **Innovative approach**
- **no significant signal was observed**
- the observed upper limit was 4.1×10^{-5} at 90% CL
- $BR(B^+ \to K^+\nu\bar{\nu}) = [1.9^{+1.3}_{-1.3}\,(\text{stat})^{+0.8}_{-0.7}\,(\text{syst})\,] \times 10^{-5}$

Phys. Rev. Lett. 127, 181802

Good sensitivity with a small dataset

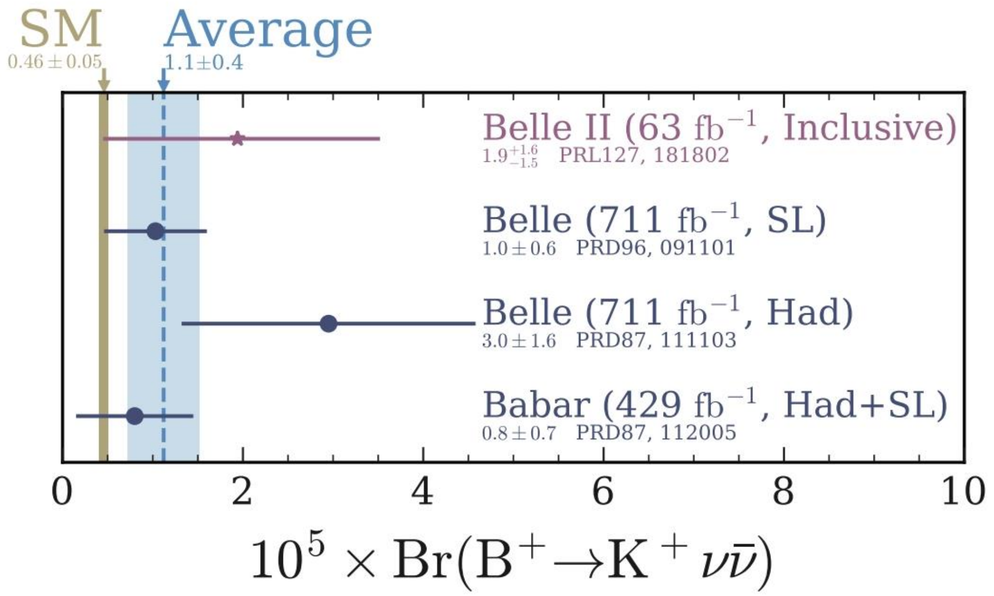

B meson tagging

Hadronic B-tagging

kinematic constraints help reconstruct signal with neutrinos in final state

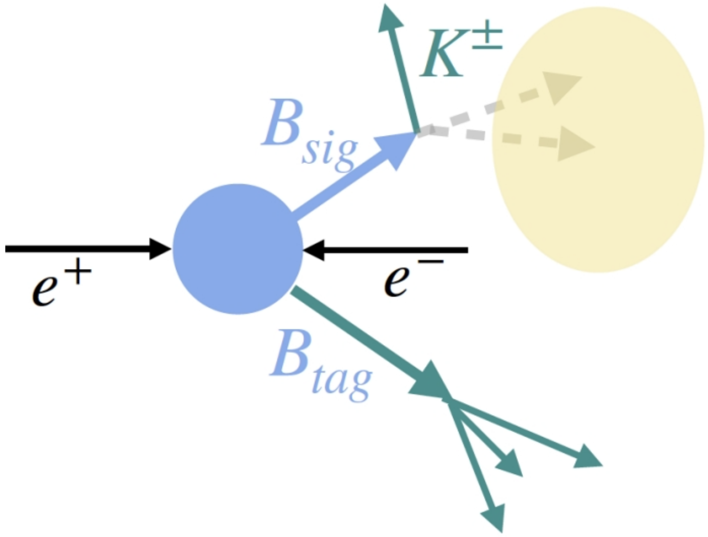

<u>Auxiliary analysis</u>

Conventional approach for B factories

Inclusive B-tagging

Only reconstruct the signal B final state, no request on the other B

Less precise reconstruction of final states with neutrinos, but **higher efficiency**

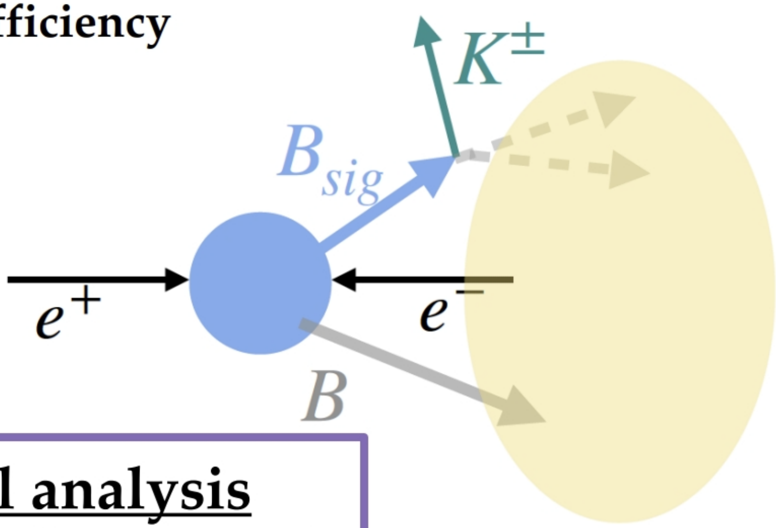

<u>Principal analysis</u>

Much larger efficiency and significantly higher sensitivity

ϵ(inc-tag) $\sim \mathcal{O}(10\%)$

ϵ(had-tag FEI) $\sim \mathcal{O}(0.1\% - 0.5\%)$

Efficiency

Purity

In a nutshell

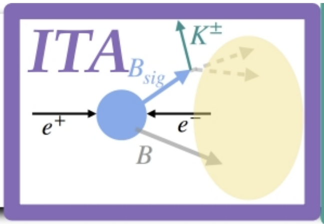

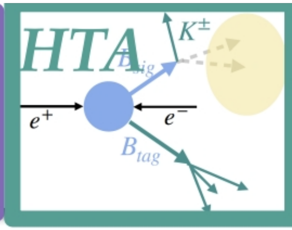

Challenges:

- Small signal rates, large background
- Two neutrinos => Under-constrained kinematics
- Continuous spectrum for the signal kaon, no good variable to fit

1) Reconstruction and basic selection

- Kaon identification
- **ITA:** reconstruct rest of the event
- ***HTA:*** reconstruct partner B in hadronic final states and rest of the event

- $\epsilon_{had-tag} \sim 0.7\ \%$
- $\epsilon_{inc} \sim 40\ \%$

2) Definition of the signal region

Cut on the output of MVA classifiers optimized and trained using simulated data

- $\epsilon_{had-tag} \sim 0.4\ \%$
- $\epsilon_{inc} \sim 8\ \%$

3) Validation

Check signal efficiency and background modeling with data

4) Signal extraction

Binned profile-likelihood fit to:

- ITA: classifier outputs and dineutrino mass
- HTA: classifier output

ITA Result

Post-fit distributions for **signal** and background

On-resonance data

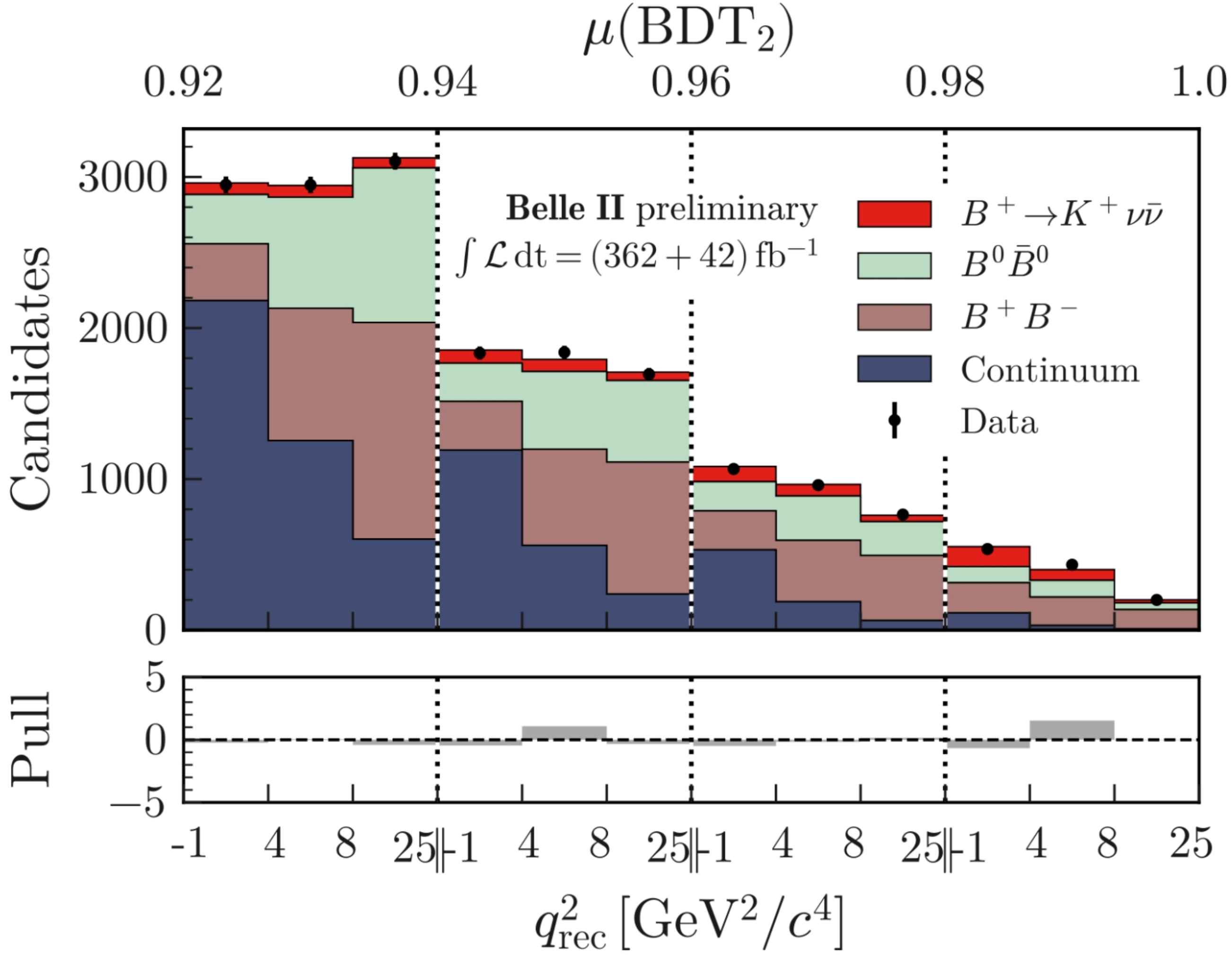

Off-resonance data

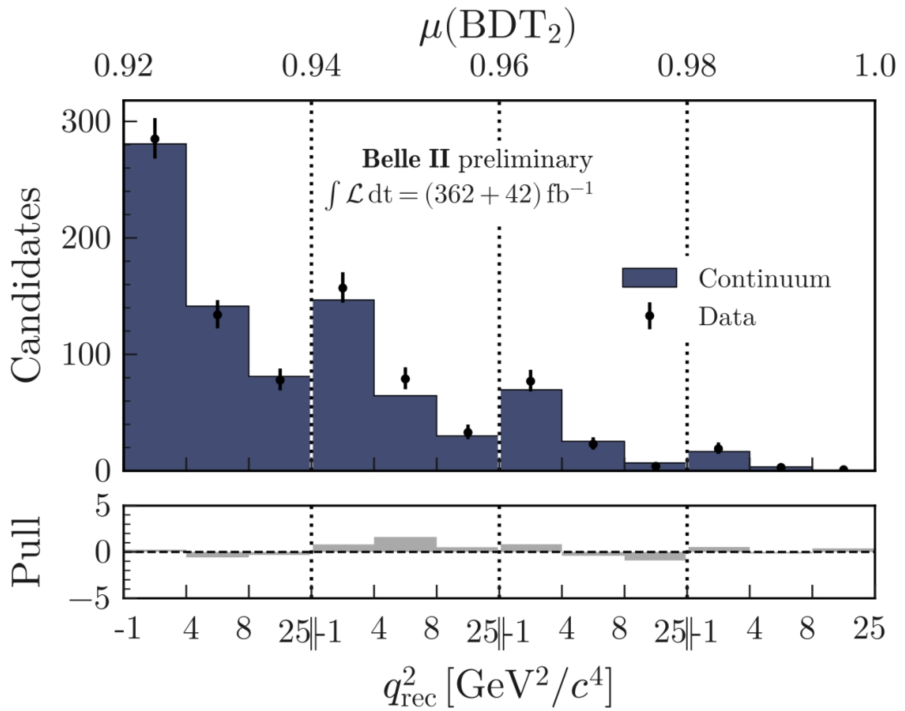

ITA Result

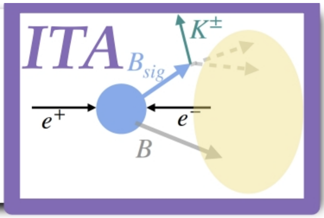

$$\mu = 5.6 \pm 1.1(\text{stat})^{+1.0}_{-0.9}(\text{syst})$$

$$\mu = BR/BR_{SM} \qquad BR_{SM} = 4.97 \times 10^{-6}$$

$$BR(B^+ \to K^+\nu\bar{\nu}) = [2.8 \pm 0.5(\text{stat}) \pm 0.5(\text{sys})] \times 10^{-5}$$

Significance of the excess with respect to the background-only hypothesis ($\mu = 0$): $3.6\ \sigma$

Significance of the excess with respect to the SM signal hypothesis ($\mu = 1$): $3.0\ \sigma$

First evidence of the $B^+ \to K^+\nu\bar{\nu}$ process

HTA Result

$$\mu = 2.2 \pm 2.3(\text{stat})^{+1.6}_{-0.7}(\text{syst})$$

$$\mu = BR/BR_{SM}$$

$$BR(B^+ \to K^+\nu\bar{\nu}) = [1.1^{+0.9}_{-0.8}(\text{stat})^{+0.8}_{-0.5}(\text{sys})] \times 10^{-5}$$

Significance with respect to the
background-only hypothesis ($\mu = 0$): 1.1σ
with SM signal ($\mu = 1$): 0.6σ

consistent with ITA:

difference in μ for ITA and HTA within 1.2 standard deviations

Post-fit distributions for **signal** and background

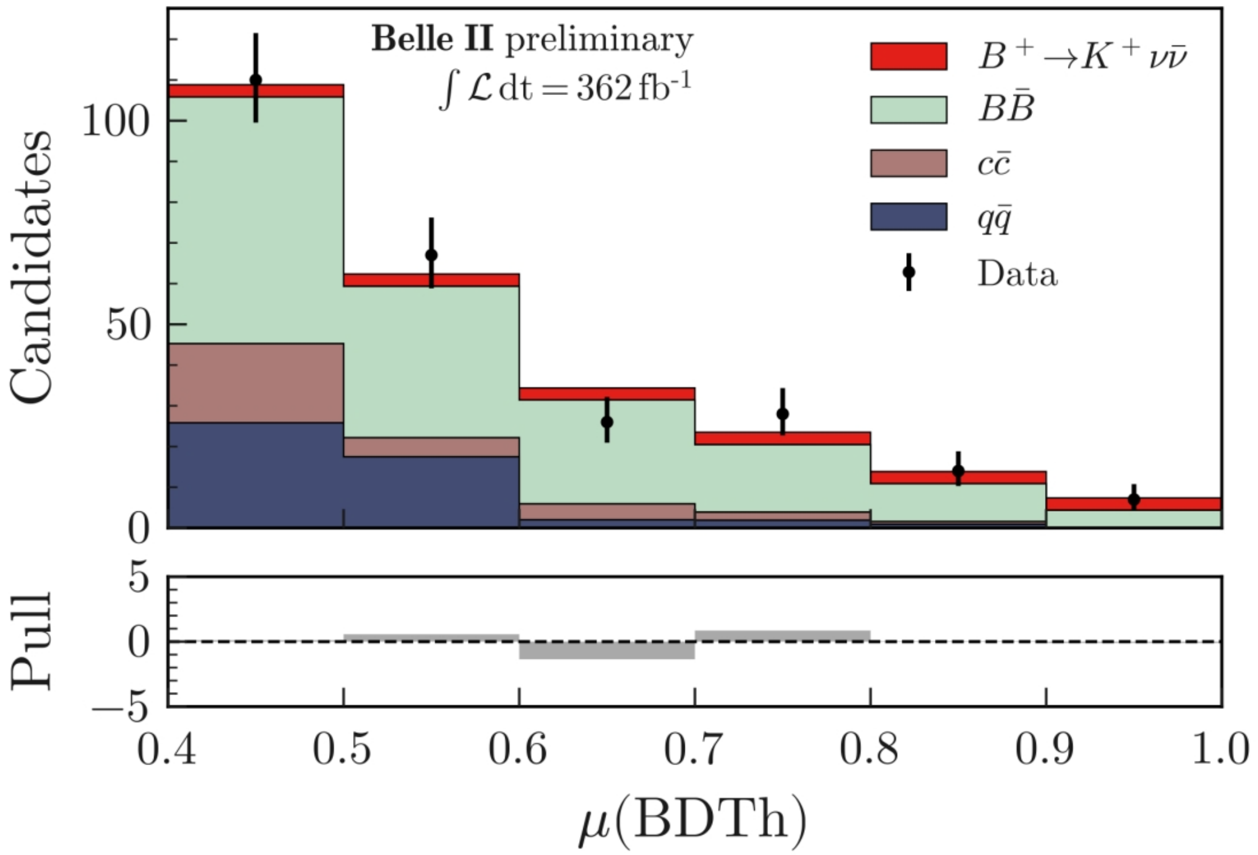

Combination

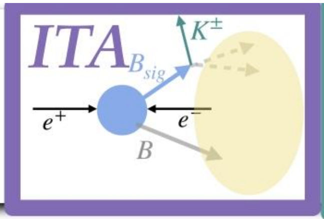

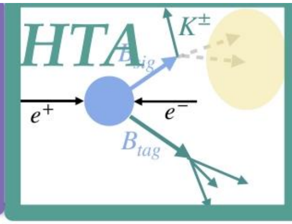

- **Consistency between ITA and HTA**
- Events from the HTA signal region represent only 2% of the signal region ITA

- Correlations among common systematic uncertainties included
- Common data events excluded from ITA sample

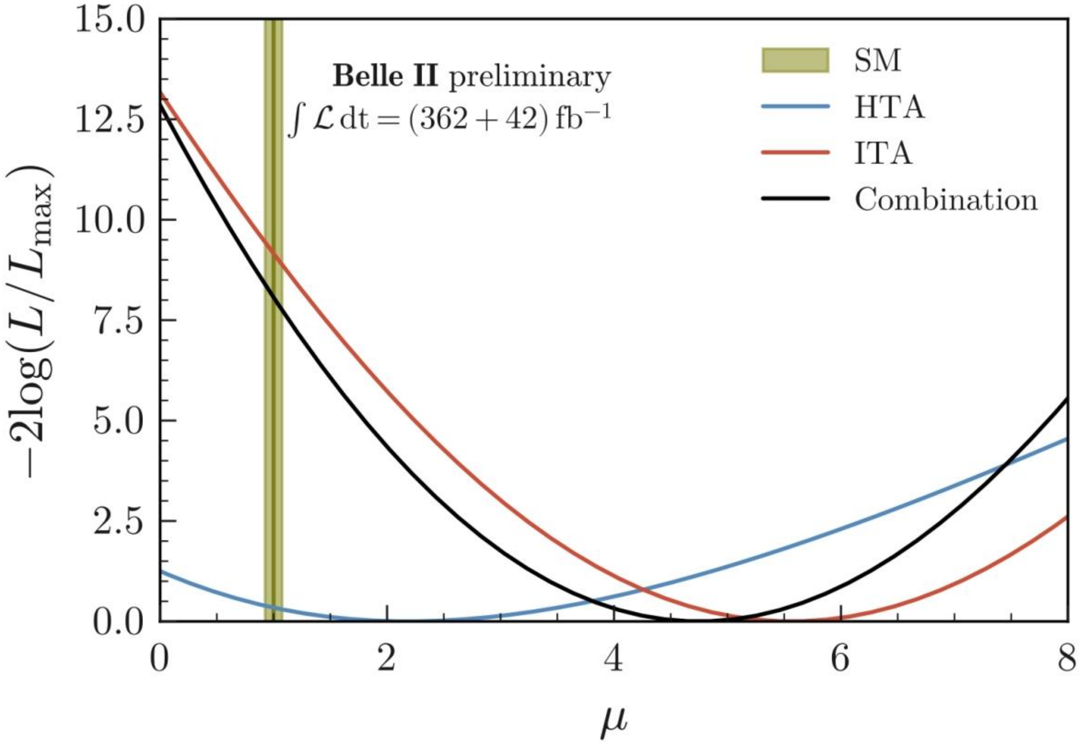

$$\mu = 4.7 \pm 1.0(\text{stat}) \pm 0.9(\text{syst})$$

$$BR(B^+ \to K^+\nu\bar{\nu}) = [2.4 \pm 0.5(\text{stat})^{+0.5}_{-0.4}(\text{sys})] \times 10^{-5}$$

ITA-HTA combination **improves the ITA-only precision by 10%**

3.6σ **Significance of the excess with respect to the background-only hypothesis ($\mu = 0$)**

First evidence of the $B^+ \to K^+\nu\bar{\nu}$ process

2.8σ **with respect to the SM signal ($\mu = 1$)**

New experimental state of the art

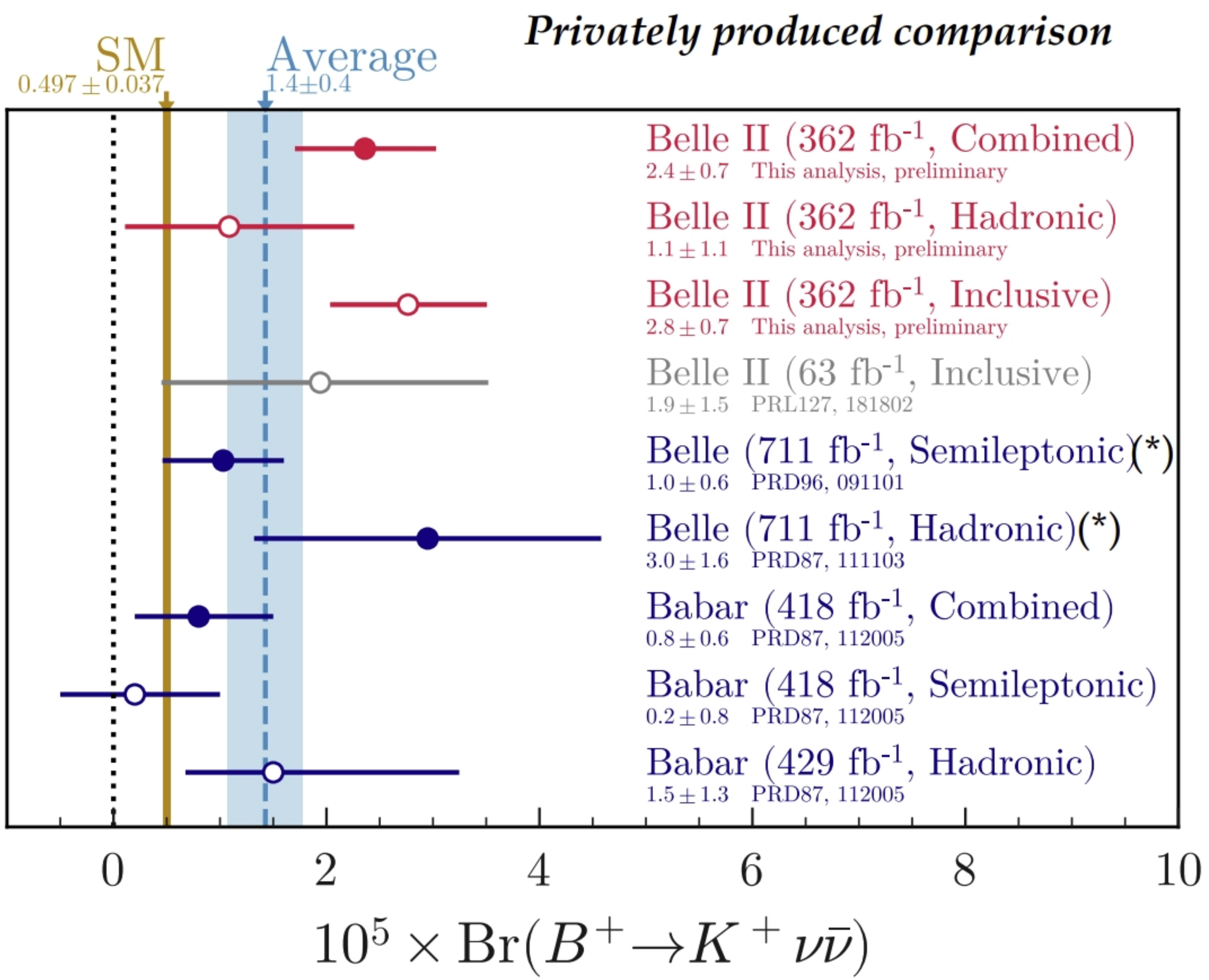

ITA result has some tension with previous semi-leptonic tag measurements
a 2.4σ tension with BaBar
a 1.9σ tension with Belle

HTA result in agreement with all the previous measurements

Overall compatibility is good: $\chi^2/ndf = 4.3/4$

(*) Belle reports upper limits only; branching fractions are estimated using published number of events and efficiency

Belle II run I (2019 - 2022)

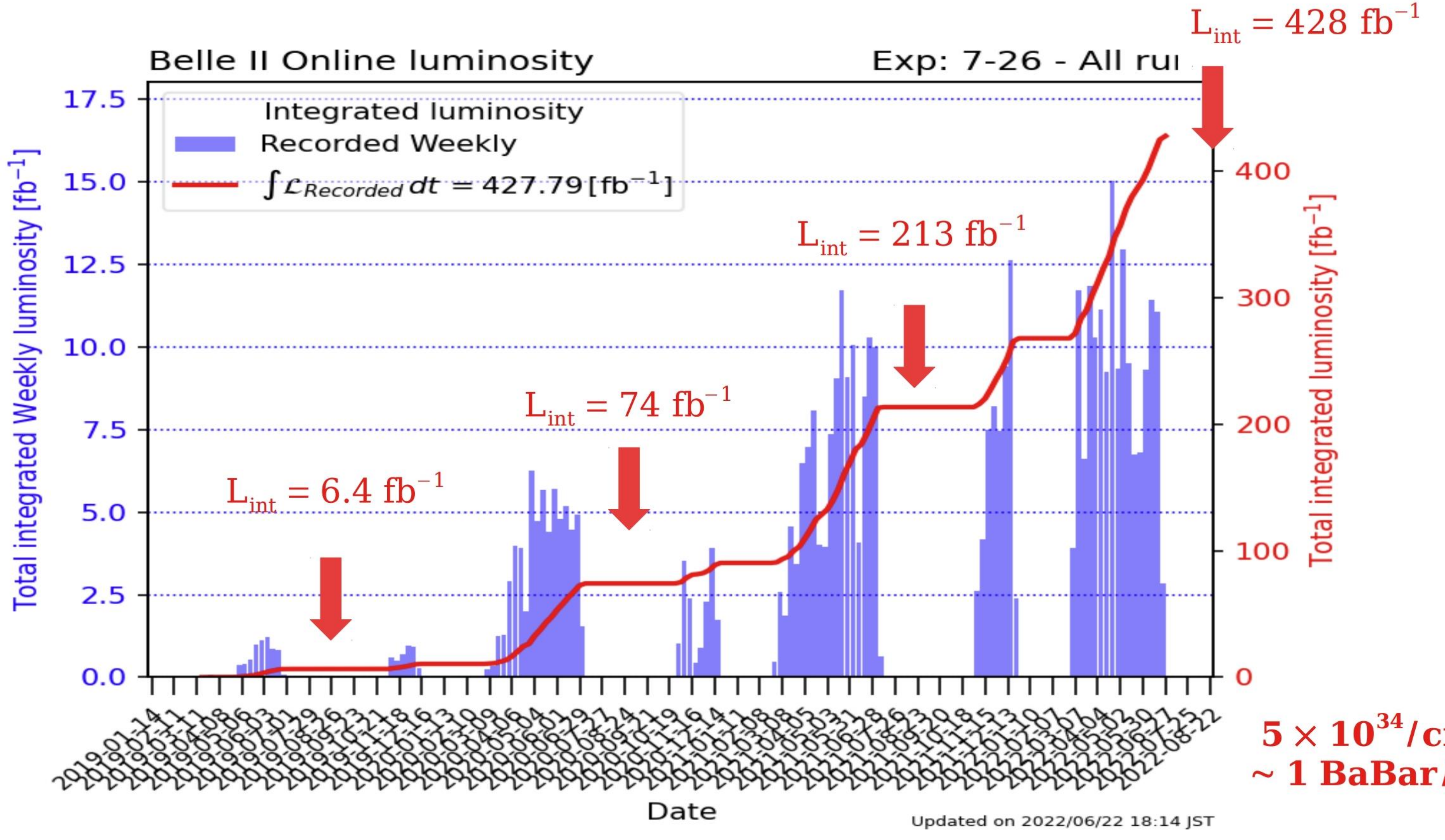

$5 \times 10^{34}/\mathrm{cm}^2/\mathrm{s}$
~ 1 BaBar/year

⇒ what about run II ?

What are our goals for 2024 ?

(please a clear and sound message)

Run stably at 10^{35}/cm^2/s

Reach 150 fb^{-1} per month

Exceed 1 ab^{-1}

(setting the pace for run 2)
(while doing good physics and working for the upgrade)

Belle II calendar

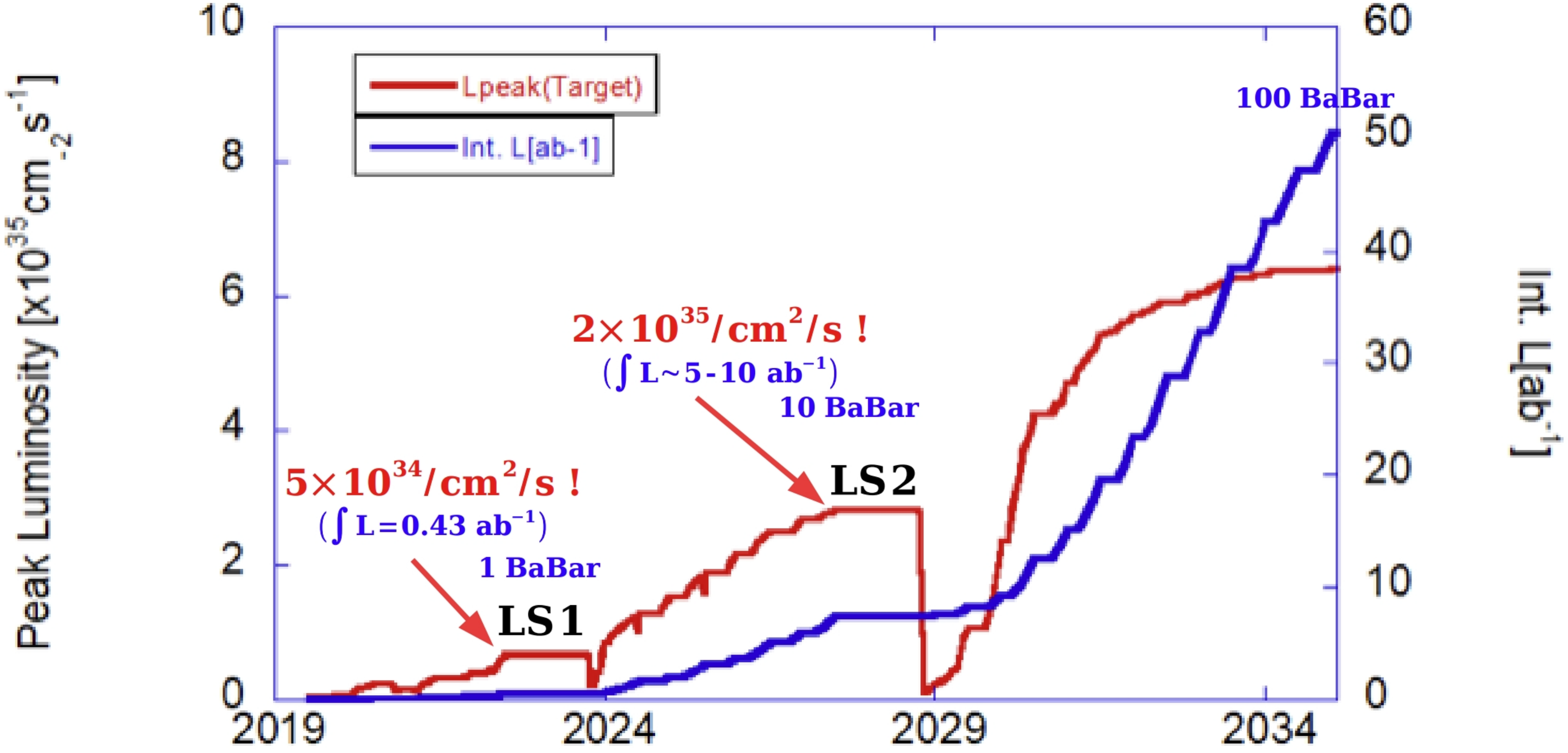

run 1 (→ June 2022): integrated luminosity ~0.43 ab^{-1}, 4-5×10^{34}/cm^2/s
PXD complete (2 layers) to be installed during **LS1** (2022-2023)
(+beampipe + TOP PMTs)

run 2 (→ 2027): integrated luminosity 5-10 ab^{-1}, 2×10^{35}/cm^2/s

2028: collider upgrade (QCS+RF) → installation upgraded detector

run 3 (→ 2035): 50 ab^{-1}

Summary

- Some new results from scan data around 10.75 GeV from Belle II come out
- We have some new results on charmed baryons from Belle
- First evidence for the $B^+ \to K^+ \nu \bar{\nu}$ decay was obtained at Belle II

- Many new results at Belle II are promising

Thanks for your attention!

Backup slides

Comparison of $\sigma_{b\bar{b}}$ and $\sigma_{B\bar{B}} + \sigma_{B\bar{B}^*} + \sigma_{B^*\bar{B}^*}$

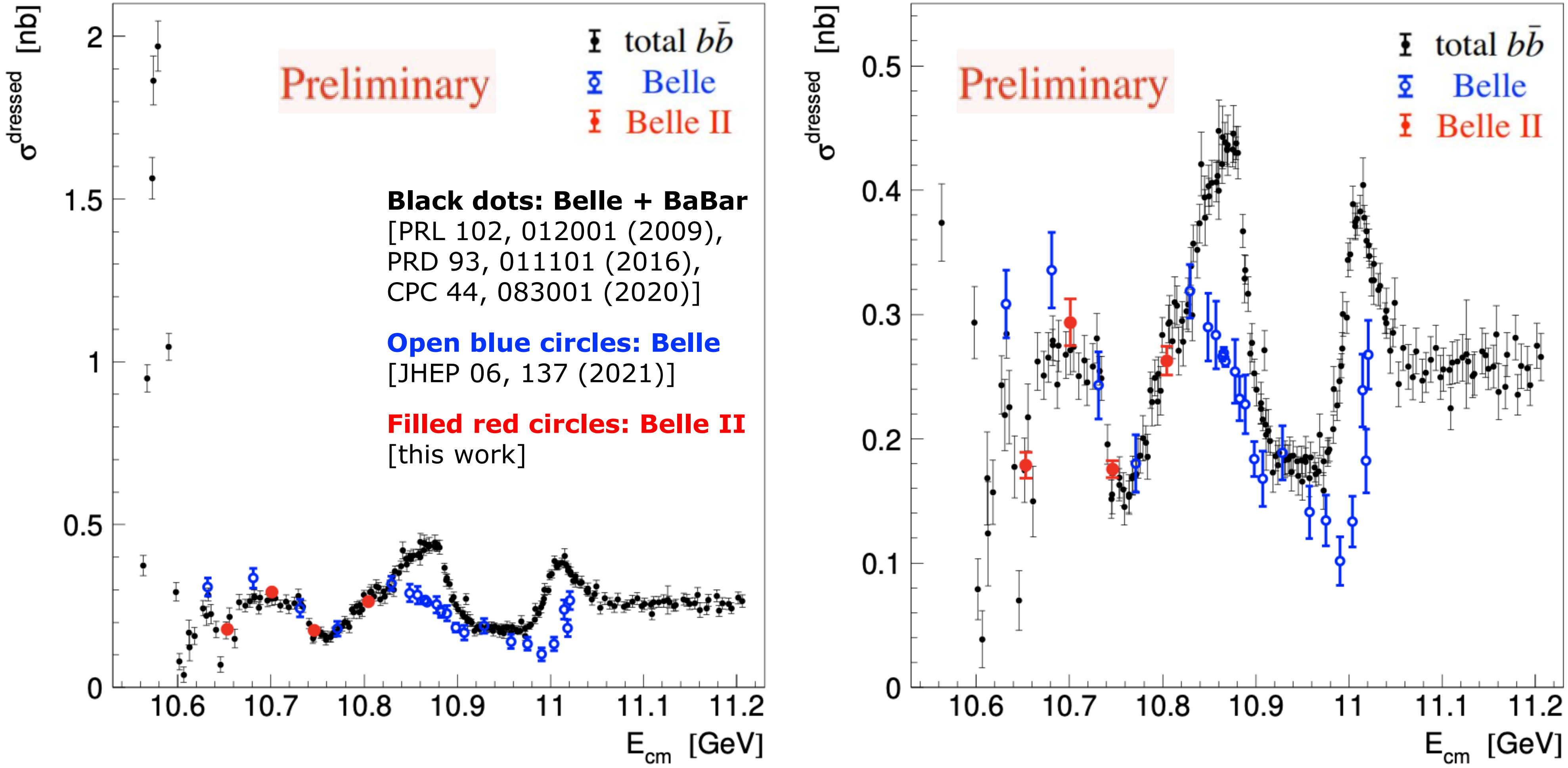

- Agreement at low energy
- Departure at high energy is due to $B_s^{(*)}\bar{B}_s^{(*)}$, multi-body $B^{(*)}\bar{B}^{(*)}\pi(\pi)$, and bottomonia

Invariant mass distribution of $\pi^+\pi^-\pi^0$

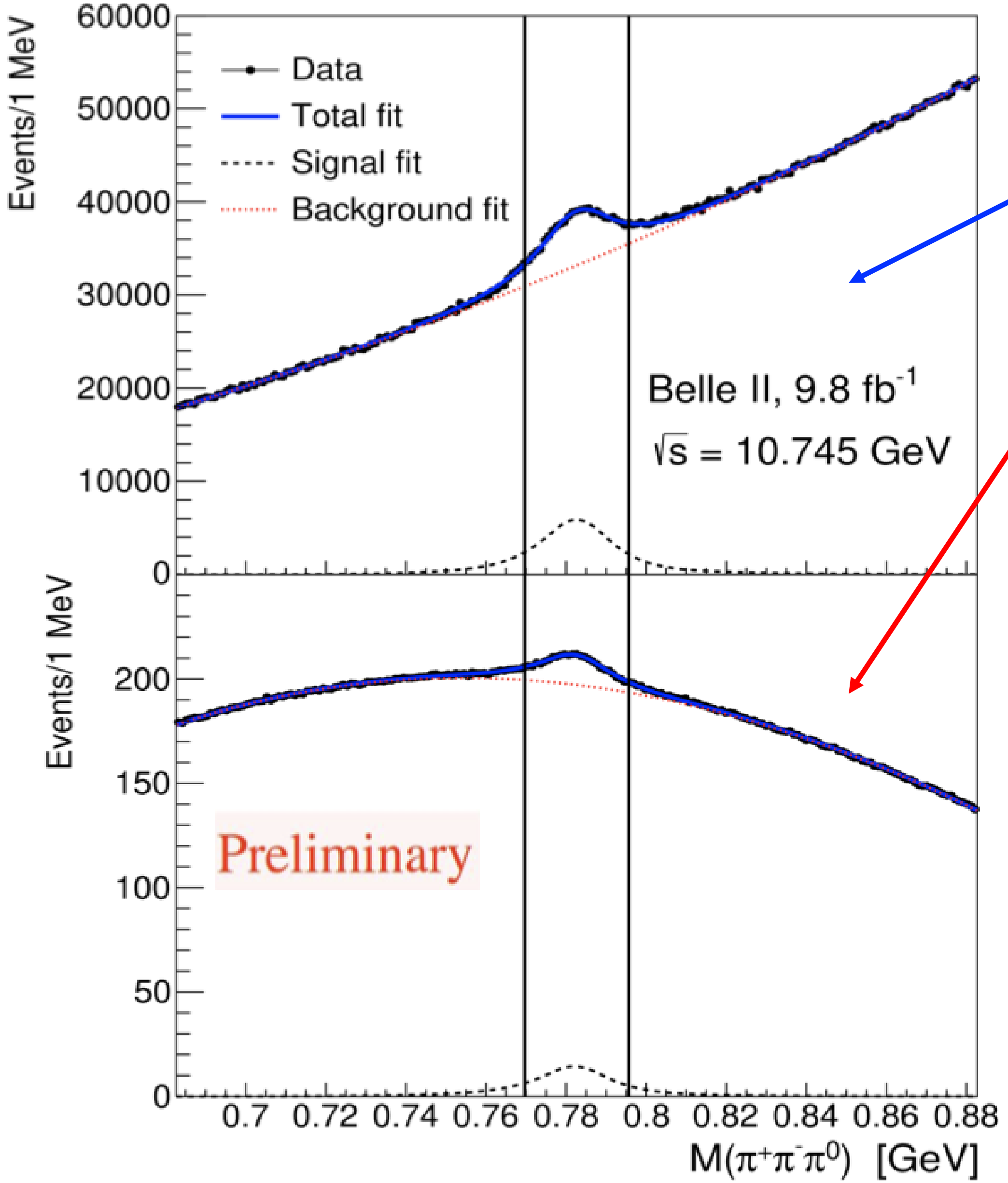

$9.2 < M_{rec}(\pi^+\pi^-\pi^0) < 9.6$ GeV/c² ($\eta_b(1S)$ included)

$9.78 < M_{rec}(\pi^+\pi^-\pi^0) < 9.95$ GeV/c² ($\chi_{bJ}(1P)$ included)

- A double-sided Crystal Ball + a Gaussian for ω signal
- 2^{nd} or 3^{rd} order Chebyshev polynomials for backgrounds
- The purities of ω-meson signals are 12.9% for $\eta_b(1S)$ and 5.3% for $\chi_{bJ}(1P)$

Bottomonium(-like) prospects at Belle II

Four ways to access bottomonia:

- Direct production from e^+e^-: $J^{PC} = 1^{--}$: $\Upsilon(nS)$
- ISR production: $J^{PC} = 1^{--}$: $\Upsilon(nS)$
- Hadronic transitions from $\Upsilon(nS)$ through η, $\pi\pi$, …

$J^{PC} = 0^{-+}, 1^{--}, 1^{+-}$ … : $\Upsilon(nS)$, $\eta_b(nS)$, $h_b(nS)$, …

- Radiative transitions from $\Upsilon(nS)$

$J^{PC} = 0^{-+}, 0^{++}, 1^{++}, 2^{++}$: $\eta_b(nS)$, $\chi_b(nP)$

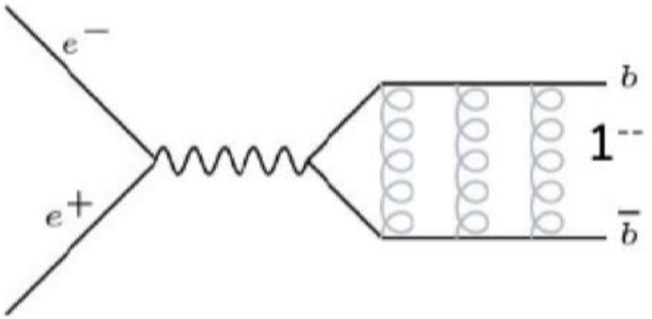

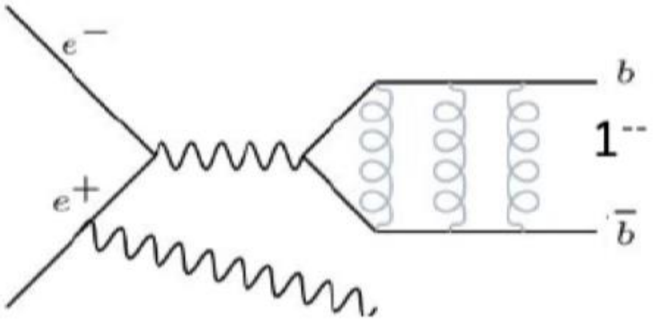

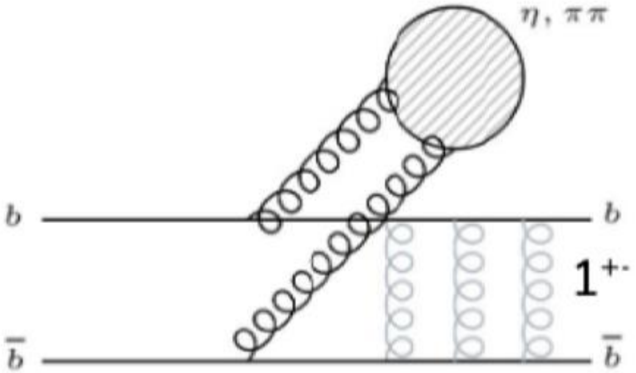

Bottomonium(-like) prospects at Belle II

Run at Υ(6S) and Υ(5S) and high energy scan:

- Search for new missing bottomonia $\eta_b(3S)$, $h_b(3P)$, $\Upsilon(D)$, exotic states Y_b, Z_b, etc
- Improve precision of already known processes and states, e.g., Z_b
- Measure the effect of the coupled channel contribution
- Study $B^{(*)}\bar{B}^{(**)}$ and $B_s^{(*)}B_s^{(**)}$ threshold regions (challenging for Super-KEKB)

Run at Υ(3S) and Υ(2S):

- Search for missing $\pi\pi/\eta$ transitions in inclusive decays to constrain further models
- Search for new physics: LFV, LFU, light Higgs, …

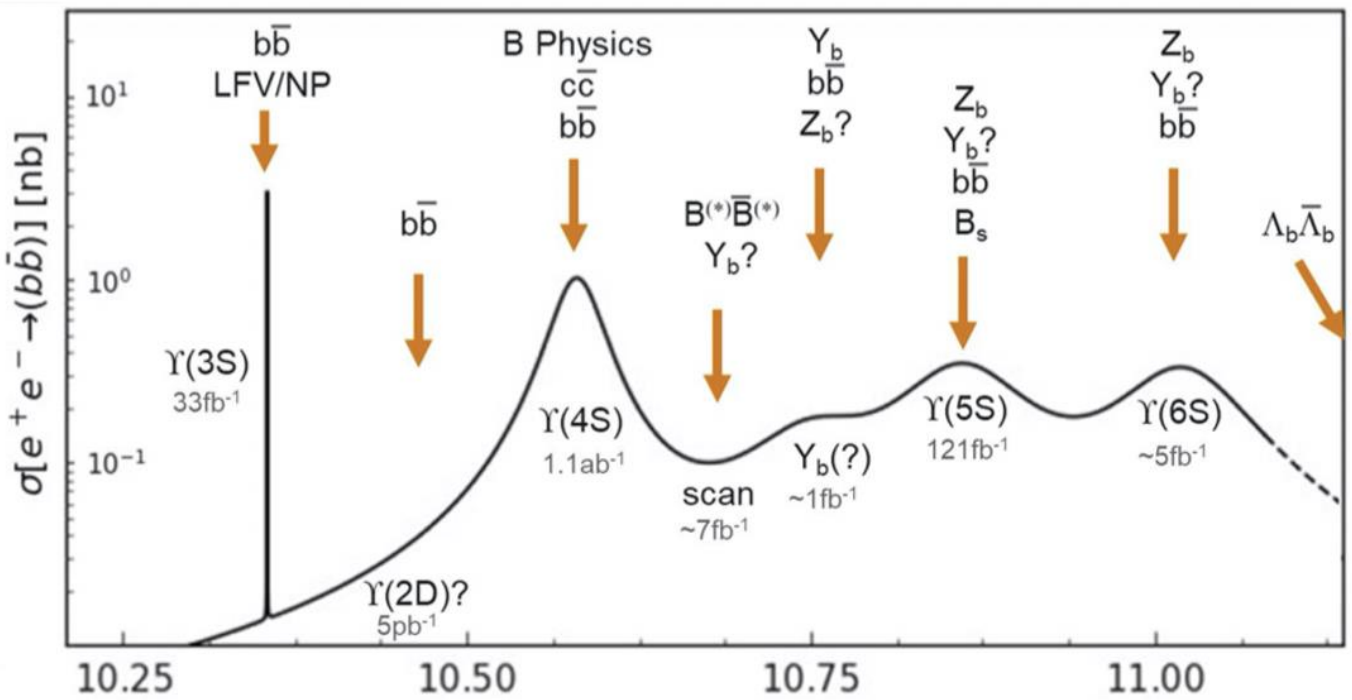

ITA Post fit distributions

Examples:

Signal region

$\mu(BDT_2) > 0.92$

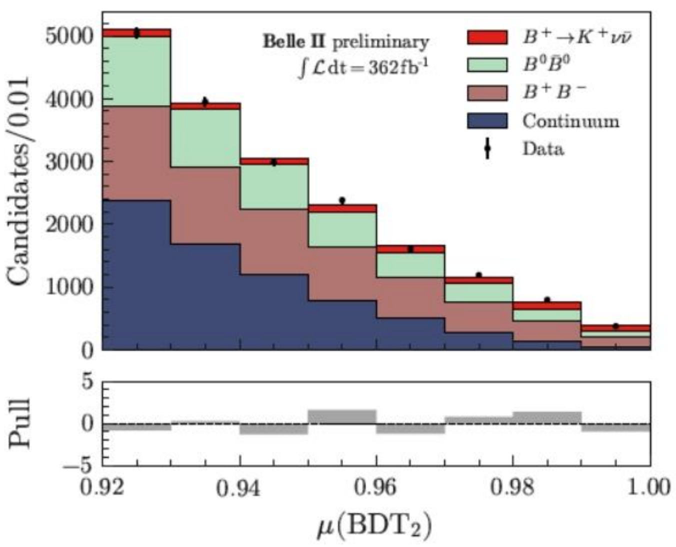

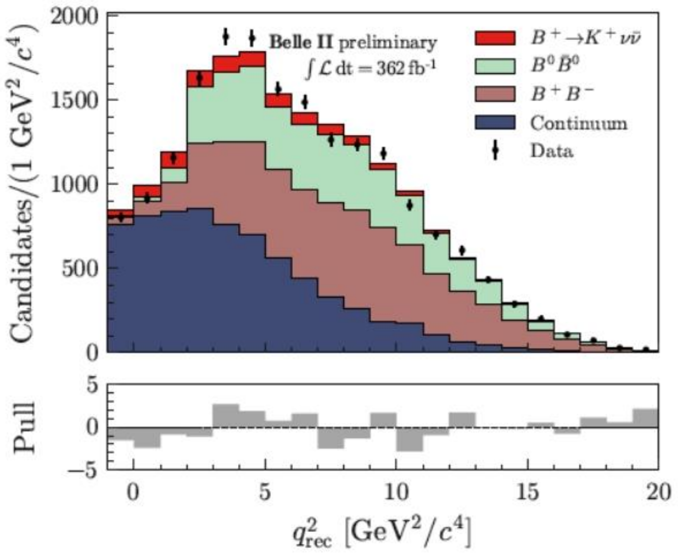

High sensitivity bins of the signal region

$\mu(BDT_2) > 0.98$

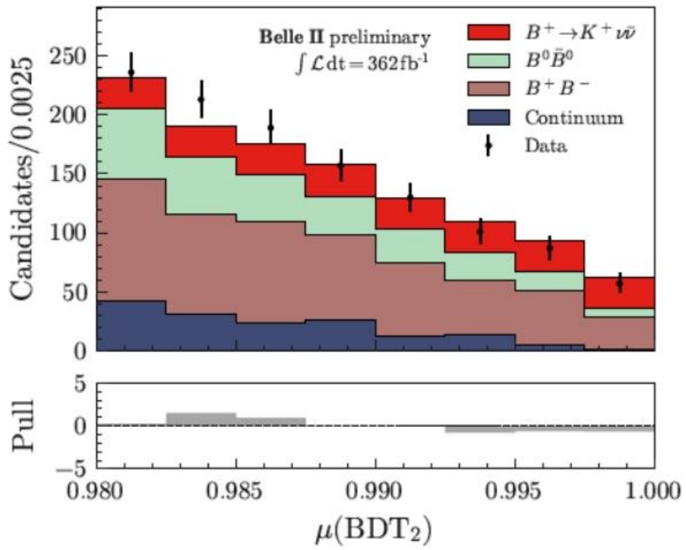

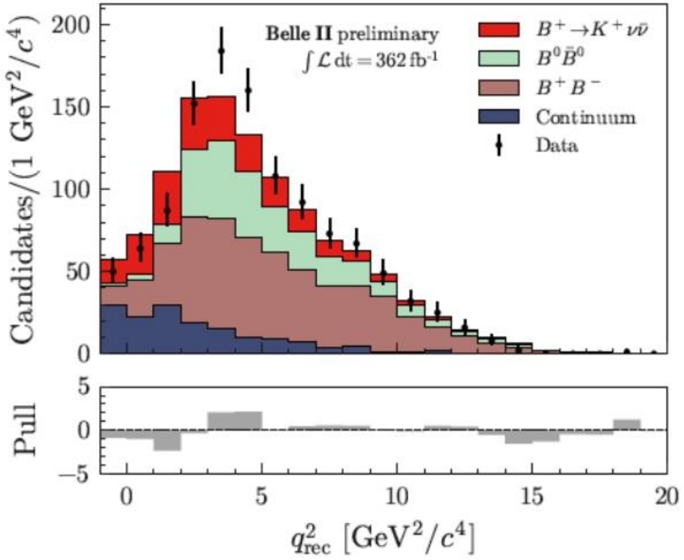

HTA Post fit distributions

Examples:

HTA Signal region $\mu(BDT_h) > 0.4$